Natural Product Reports

ROYAL SOCIETY OF CHEMISTRY

REVIEW

View Article Online
View Journal | View Issue

Cite this: *Nat. Prod. Rep.*, 2023, **40**, 718

Natural sesquiterpene quinone/quinols: chemistry, biological activity, and synthesis†

Xin-Hui Tian, [ab] Li-Li Hong, [a] Wei-Hua Jiao [a] and Hou-Wen Lin *[a]

Covering: 2010 to 2021

Sesquiterpene quinone/quinols (SQs) are characterized by a C15-sesquiterpenoid unit incorporating a C6-benzoquinone/quinol moiety. Numerous unprecedented carbon skeletons have been constructed with various connection patterns between the two parts. The potent anti-cancer, anti-inflammatory, anti-microbial, anti-viral, and fibrinolytic activities of SQs are associated with their diverse structures. The representative avarol has even entered the stage of clinical phase II research as an anti-HIV agent, and was developed as paramedic medicine against psoriasis. This review provides an overall summary of 558 new natural SQs discovered between 2010 and 2021, including seven groups and sixteen structure-type subgroups, which comprehensively recapitulates their chemical structures, spectral characteristics, source organisms, biological activities, synthesis, and biosynthesis, aiming to expand the application scope of this unique natural product resource.

Received 29th June 2022

DOI: 10.1039/d2np00045h

rsc.li/npr

[a]*Marine Drugs Research Center, Department of Pharmacy, Ren Ji Hospital, School of Medicine, State Key Laboratory of Microbial Metabolism, Shanghai Jiao Tong University, Shanghai 200127, P. R. China. E-mail: franklin67@126.com*

[b]*Institute of Interdisciplinary Integrative Medicine Research, Shanghai University of Traditional Chinese Medicine, Shanghai 201203, P. R. China. E-mail: tianxinhui@126.com*

† Electronic supplementary information (ESI) available. See DOI: https://doi.org/10.1039/d2np00045h

1. Introduction

Terpenoid quinone/quinols, which are generally known as meroterpenoids, are hybrids of terpenoids and quinone/quinols. Sesquiterpene quinone/quinols (SQs) are the most common meroterpenoids found in nature. They have unique frameworks due to the structural variation of the sesquiterpene and quinone/quinol moieties, and varied connection patterns between the two units. Most of these compounds may be derived from polyketide synthase- and terpenoid synthase-mediated biosynthetic pathways, and others may be derived from shikimate-terpenoid adducts, which are the most common type of non-polyketide-derived meroterpenoids.[1,2] SQs exhibit potent biological activities related to the redox characteristics and electron transfer function of the quinone/quinol group, and the hydrophobic–hydrophilic balance of the sesquiterpenoid unit. For example, avarol from *Dysidea avara* exhibits anti-HIV, anti-leukemic, and anti-parasitic activities, and has been used as paramedic medicine against psoriasis by the German company KliniPharm.[3–10] Ilimaquinone from *Hippospongia metachromia* induces Golgi vesiculation and fragmentation, which may be closely related to its diverse biological activities, including anti-HIV, cytotoxic, anti-

Xin-Hui Tian received her PhD degree in pharmacognosy from Peking Union Medical College in 2012. She continued as a post-doc at Second Military Medical University, where she focused on the terpenoid constituents of Illicium merrillianum. *Then she joined Shanghai University of Traditional Chinese Medicine as a research assistant, where she has remained to date. In 2021, she joined the research group of Professor Hou-Wen Lin as a visiting scholar and studied the structure and biological activity of sesquiterpene quinone/quinols from marine resources.*

Wei-Hua Jiao initially studied plant alkaloids (Master and PhD Prof Xin-Sheng Yao, Shenyang Pharmaceutical University) but marine natural products became a major focus after joining Prof. Hou-Wen Lin's research group in Second Military Medical University. He became a research assistant professor at Research Center of Marine Drugs, Ren Ji Hospital, School of Medicine, Shanghai Jiao Tong University in 2013. After a two-year visiting academic and post-doctoral fellowship at the University of Queensland with Prof. Robert J. Capon, Australia, he returned to Shanghai Jiao Tong University in 2017, where he is now a professor. He is currently a visiting professor in the research group of Prof. Helge B. Bode at Max Planck Institute for Terrestrial Microbiology, Marburg, Germany. His research involves the discovery and development of new bioactive natural products from marine invertebrates and microbes.

Li-Li Hong obtained a PhD degree in pharmacy from Shanghai Jiao Tong University in 2017. Next, she held a post-doctoral appointment with Professor Hou-Wen Lin, and then worked as a research assistant at Renji Hospital, affiliated to Shanghai Jiao Tong University School of Medicine. Her current research mainly focuses on the discovery of bioactive natural products from marine sponge-derived microorganisms.

Hou-Wen Lin received his PhD degree in Marine Natural Product Chemistry from Shenyang Pharmaceutical University in 1998 under the supervision of Prof. Xin-Sheng Yao and Prof. Yang-Hua Yi, and did his joint research at Kanagawa University, Japan. He served as a pharmacist at Shanghai Changzheng Hospital from 2000, and was promoted to a Director & Professor in 2008 and awarded the "National Science Fund for Distinguished Young Scholars" in 2012. In 2013, he relocated to Shanghai Jiao Tong University as a "National Yang-Zi River Scholar" in Marine Drugs. His scientific interests focus on the discovery, synthesis, biosynthesis, and mechanisms of bioactive metabolites from marine sponges and their microbial symbionts.

inflammatory, and anti-microbial properties.[11–16] These natural SQs have proven to be significant resources for drug discovery. Marcos *et al.* and Capon reviewed the structure, bioactivities, source organisms, and stereochemical investigations of marine-derived SQs in 1995 and 2010, respectively.[17,18] During the past decade, an increasing number of new SQs have emerged due to rapid advances in discovery methods, such as genome mining, biotransformation, microbial co-culture, chemistry first and MS/MS-based molecular networking, and fluorescent image-based high-content screening techniques, fast-growing improvement in analytic techniques such as NMR, MS, and single crystal X-ray diffraction, and great progress in diving equipment and collection tools used for marine organisms and microorganisms.[19–29] However, there have been no systematic reviews on these newly discovered SQs, and there are only some reviews on meroterpenoids that cover part of the SQ family.[30–32]

In this article, we provide 558 new SQs discovered during 2010–2021 and comprehensively describe their source organisms, chemical structure, bioactivities, and synthesis. SQs are extensively distributed in marine sponges, algae, ascidians, coral, fungi, and plants (Fig. 1). The metabolites from marine and marine-derived fungi account for 60.2% of the total SQs, and sponges are the predominant sources, producing 38.0% of these SQ metabolites. The fungi of *Stachybotrys* sp. and *Ganoderma* sp. produced 130 and 82 new compounds, respectively, and the sponge of *Dysidea* sp. produced 84 new compounds, ~53% of the total number of SQs, which is the hottest research target.

These natural SQs are divided into seven groups and sixteen subgroups based on the skeletons of the sesquiterpenoid subunits (Fig. 2), including five groups for drimane-type (tauranin-type, phenylspirodrimane-type, chrodrimanin-type, dasyscyphin-type, and hymenopsin-type), five groups for avarane-type (typical avarane-type, dactyloquinone-type, dysideanone-type, spiroetherane-type, and dysidavarane-type), four groups for monocyclofarnesane type (cochlioquinone-type, metachromiane-type, bisabolane-type, and tricycloalternarene-type), and two groups for dimer-type (true and pseudo SQ-dimers). The drimane-type (118 compounds, 21%), avarane-type (152, 27%), and farnesane-type (134, 24%)

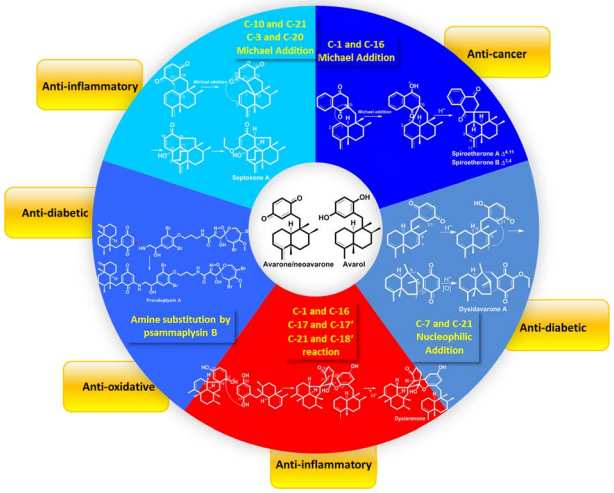

Fig. 1 The distribution of sesquiterpene quinone/quinols (SQs) in Nature.

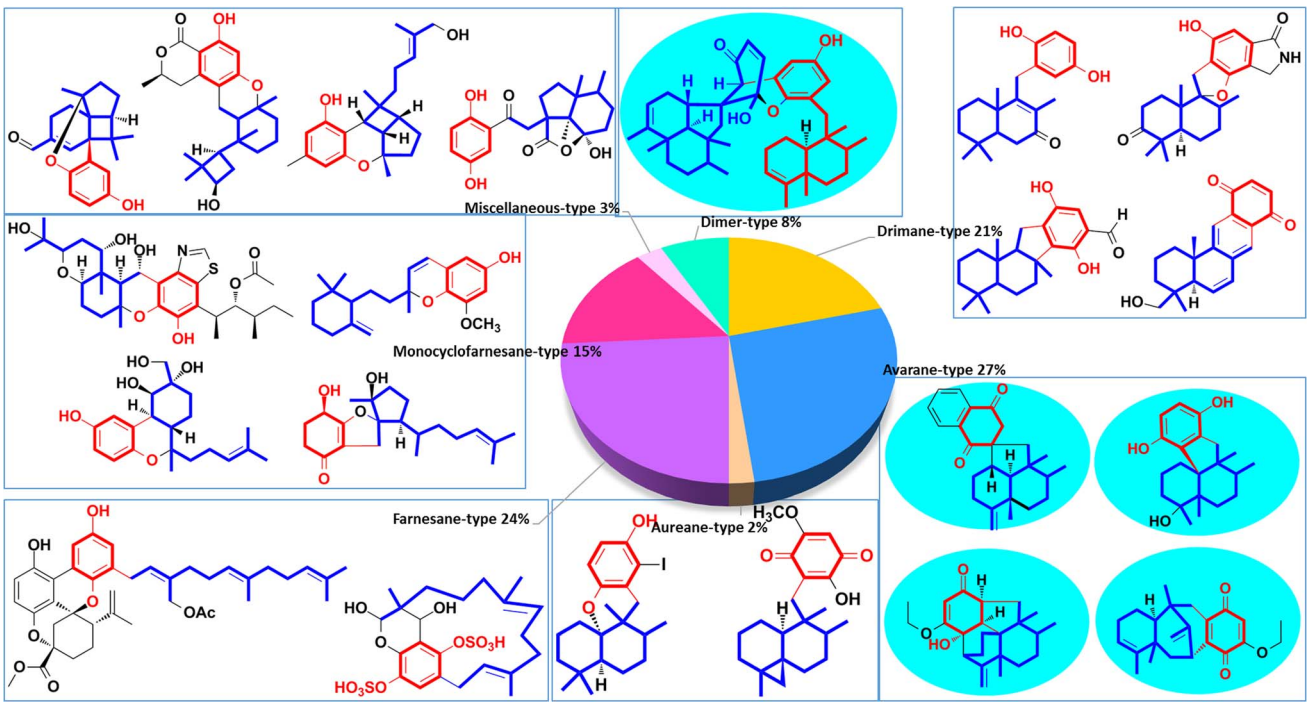

Fig. 2 Proportion of sesquiterpene quinone/quinols with different types of skeletons.

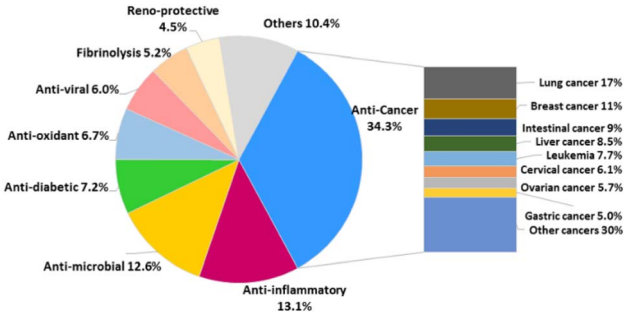

Fig. 3 Proportion of each activity compared to the whole occurrence of activities observed for sesquiterpene quinone/quinols isolated from nature.

comprise an enormous proportion of SQs, followed by monocyclofarnesane-type (83, 15%) and dimer-type (47, 8%). Avarane-type SQs only exist in marine sponges, and more than half have been reported from *Dysidea* sp. The dysideanone-, septosone-, dysidavarane, dysiarenone-, and spiroetherane-type SQs in the blue shadow of Fig. 2 were all discovered from *Dysidea* sponge by H. W. Lin's group.[33–37] The SQ second metabolites of fungi include drimane-, aureane-, farnesane-, monocyclofarnesane-, bisabolane-, and dimer-type. Most phenylspirodrimanedrimane-type analogs are isolated from the genus *Stachybotrys*, about half of the farnesane-type and all bisabolane-type analogues are reported from the genus *Ganoderma*.

Pharmaceutical studies have indicated that 48% of SQs were biologically active with ~34.3% of the active compounds (268 compounds) displaying anti-cancer activity, followed by anti-inflammatory (13.1%), anti-microbial (12.6%), anti-diabetic (7.2%), anti-oxidant (6.7%), anti-viral (6.0%), reno-protective (5.2%), fibrinolysis (4.5%), and other (10.4%) activities (Fig. 3). The anti-cancer SQs are more active toward lung cancer cells (17%), breast cancer cells (11%), intestinal cancer cells (9%), liver cancer cells (8.5%), leukemia cells (7.7%), cervical cancer cells (6.1%), ovarian cancer cells (5.7%), and gastric cancer cells (5.0%) (Fig. 3). The anticancer and fibrolytic activities seem to be more attractive and visible. Thus, many *in vivo* and *in vitro* activity and mechanistic studies have been carried out. However, further biological studies on many promising new drug candidates have been limited due to the scarcity of samples obtained from natural resources. The chemical synthetic and biosynthetic routes outlined in this review will provide inspiration for synthetic design and enhance the understanding of the biomedical potential and biosynthetic logic of SQs.

2. Structures, classifications, and distributions of natural SQs

We have classified SQs into seven groups, five of which have a unified sesquiterpenoid skeleton, one type consists of miscellaneous sesquiterpenoid skeletons, and the last type consists of SQ dimers. Some groups of SQs contain subtypes because new carbon skeletons are built when the sesquiterpenoid and quinone units are connected in different ways. We have summarized advanced discovering techniques, common structural characteristics, and typical NMR, MS spectral signals for each type of SQs, which will help researchers efficiently recognize the unknown constituents. The determination of the absolute stereochemistry of SQs has also been included because it is crucial for their bioactivity and further synthetic design.

2.1. Drimane-type SQs

Drimane-type SQs are the most common structures found in nature, and the sesquiterpene unit features a drimane skeleton containing *trans*- or *cis*-fused ring junctions. They contain five subtypes including tauranin-type, phenylspirodrimane-type, chrodrimanin-type, dasyscyphin-type, and hymenopsin-type based on the connection modes between drimane and the C-6 benzene moiety.

2.1.1. Tauranin-type SQs. The earliest tauranin-type natural SQs were isolated from the mold Oospora aurantia in 1964.[38] Tauranin-type SQs are structures in which the drimane connects with the benzene quinone/quinols *via* the C-1′–C-14 bond. Fungi-derived SQs are characterized by a methylol or aldehyde substituent at C-4′ and usually by the oxidation of the double bond on the benzoquinone unit, such as purpurogemutantin (**1**) and purpurogemutantidin (**2**), penicilliumin A (**3**), myothecols A–H (**4–11**), craterellins A–D (**12–15**), compound **16**, 2′,3′-epoxy-13-hydroxy-4′-oxomacrophorin A (**17**), neomacrophorins I–III (**18–20**), epoxyphomalins C–E (**21–23**), and pleosporallins A–D (**24–27**) from sponge, alga, and plant-derived fungi of *Penicillium* sp., *Myrothecium* sp., *Craterellus odoratus*, *Phialocephala* sp., *Hymenopsis* sp., *Trichoderma* sp., *Paraconiothyrium* sp., *Lophiostoma* sp., and *Pleosporales* sp.[39–50] Craterellin A (**12**) has been detected in both *Lophiostoma* sp. and *Craterellus odoratus*, indicating the close relationship between the two species.[44,45] Peyssonoic acid A (**28**) was the first report of a C-4′ acetic acid-substituted SQ isolated from the marine macroalga *Peyssonnelia* sp.[51] The macroalga *Gracilaria salicornia* produces 13-[[2-(hexyloxy)-2,5,5,8*a*-tetramethyldecahydro-1-naphthalenyl](methoxy)methyl] benzenol (**29**).[52] Cell lysis-guided chromatographic fractionation of the extract from *Dictyopteris undulata* has led to the identification of zonarenone (**30**) and isozonaroic acid (**31**).[53,54] The absolute configuration of **31** was established to be 5*R*, 9*R*, and 10*R* on comparing its optical rotation with that of its methyl ester, which was synthesized *via* the triflation of one hydroxy group in isozonarol, followed by palladium-catalyzed alkoxycarbonylation. Dysidphenol C (**32**) and highly polar siphonodictyal A sulfate (**33**) were identified from the marine sponges *Dysidea* sp. and *Aka coralliphaga*, respectively.[55,56]

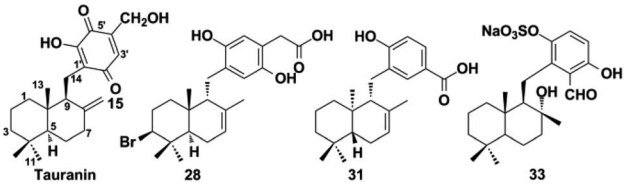

2.1.2. Phenylspirodrimane-type SQs. Phenylspirodrimane-type SQs are characterized by a spiro heterocyclic system, in which drimane is attached to the benzene moiety *via* a spirofuran ring. A hydroxyl substituent at the C-3 position is common in fungal metabolites. When CH_2-11 and methyl-15 were on the same side of the plane, the ^{1}H NMR of CH_2-11 exhibits two doublet peaks at δ_H = 2.7–3.3 ppm with J = 16–17 Hz and δ_C in the range of 30–33 ppm; the ^{13}C NMR chemical shift of CH_2-11 will move downfield significantly (δ_C = 40.0 ppm) when CH_2-11 and methyl-15 were on opposite sides of the plane.[57] These compounds were found to be the major secondary metabolites of *Stachybotrys* sp. and may be used as a chemotaxonomic marker.[58] The fungal genus *Stachybotrys* is comprised of ~100 species that are widespread in marine invertebrates, soil, and plants.[59] Among these species, *Stachybotrys chartarum* has been well studied and yielded a plethora of new SQs, including marine-derived chartarolides A–C (**34–36**), chartarlactams A, B, D, E–K, and M–P (**37–50**), stachybotrins D–F (**51–53**), stachybosides A–B (**54–55**), and stachybonoids D–F (**56–58**), soil-sample-derived stachartins A–E (**59–63**), plant-derived stachybochartins E–F (**64–65**), stachybotrysins A–G (**66–72**), and stachybotrysam E (**73**).[60–67] The sesquiterpene hydroquinone part is connected to mollicelin J to form a unique [6,6,6,6]-tetracyclic skeleton with a central [3,3,1]-bicyclic ketal core fused with two aromatic rings in **34** and **35**.[62] Compound **69** contains an unconventional sulfonic substituent.[60] Stachybosides A and B (**54–55**) were identified as the first phenylspirodrimane glucosides, and their α-D-glucopyranose group was determined using chiral separation and acid hydrolysis methods.[64] Other *Stachybotrys* sp. from marine habitats have been found to produce stachyin A (**74**), stachybotrin H (**75**), stachybotrysin H (**76**), stachybotrysin (**77**), and stachybotrylactone B (**60**).[59,68,69] It is worth mentioning that stachybotrylactone B (**60**) and stachartin B (**60**) have the same structure.[66,69] Chermesins A–D (**78–81**) from alga-derived *Penicillium chermesinum* EN-480, myrothecisins A and B (**82–83**) from plant-derived *Myrothecium* sp. OUCMDZ-2784, and stachybotrin G (**84**) from soil-derived *Stachybotrys parvispora* HS-FG-843 have been characterized by two methyl/methylene/methine substituents on the quinone/quinol moiety.[57,70,71] Phenylspirodrimane-type SQs were discovered from fungi as well as marine sponges, such as dysidphenols A–B (**85–86**) from *Dysidea* sp., cyclospongiacatechol (**87**) from *Dactylospongia elegans*.[16,55]

2.1.3. Chrodrimanin-type SQs. For the chrodrimanin-type SQs, drimane is attached to the benzene moiety *via* a pyran ring. A series of chrodrimanin-type metabolites, namely, chrodrimanins C–H (**88–93**), have been reported from the YO-2 strain of *Talaromyces* sp. by the Akiyama group.[72,73] *ent*-thailandolide B (**94**) and chrodrimanin T (**95**) have been reported in fresh water and the plant-derived fungus *Talaromyces amestolkiae*, respectively.[74,75] The reconstitution of one cryptic *fnc* gene clusters in *Aspergillus funiculosus* CBS 116.56 has led to the discovery of funiculolides A–D (**96–99**). Funiculolide (**99**) is synthesized as the end product of *fnc* cluster and has an unprecedented spirocyclopentanone system.[27] Studies on the Indonesian ascidian-derived fungal strain *Penicillium verruculosum* have revealed verruculide A (**100**).[76] The DES-mutant and

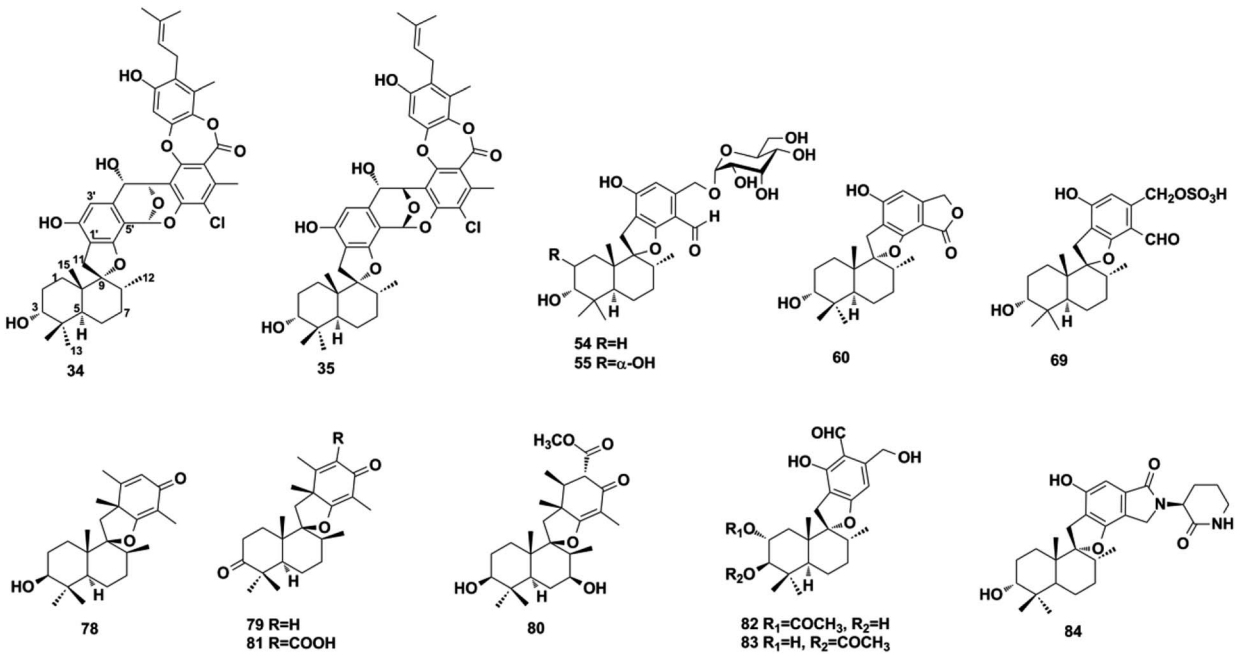

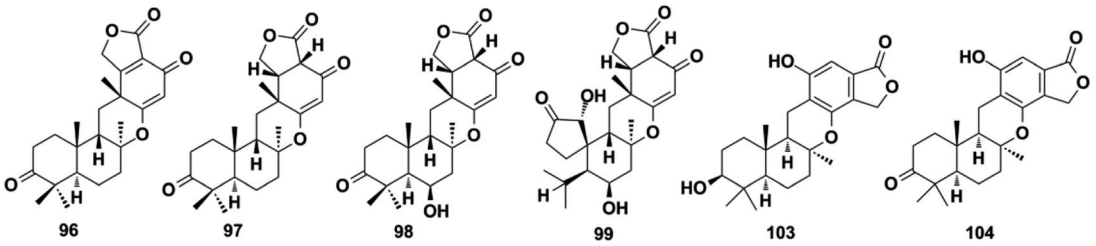

marine-derived fungus *P. chrysogenum* S-3-25 produce 3-acetyl chrodrimanin F (**101**) and 3-acetoxypentacecilide A (**102**).[28] These chrodrimanin-type metabolites may serve as significant chemotaxonomic markers used to distinguish *Talaromyces*, *Penicillium*, and *Aspergillus* fungi from other genera in the *Trichocomaceae* family. In addition, the chromatographic fractionation of the crude extract of the endophytic fungus *Phomopsis archeri* has yielded three congeners: phomoarcherins A–C (**103–105**).[77] The absolute configuration of **103** was established to be 3*S*,5*R*,8*S*,9*R*,10*S* using X-ray crystallographic analysis of its *p*-bromobenzoate derivative, which provides a reference value for the stereochemistry establishment of other pentacyclic analogs. Marine sponges have also been found to contain chrodrimanin-type SQs, such as 20-demethoxy-20-ethoxycyclospongiaquinone-1 (**106**) from *Spongia pertusa* Esper, puupehenol (**107**) from *Dactylospongia* sp., cyclosiphonodictyol A (**108**) from *Aka coralliphagum*, and 19-methoxy-9,15-ene-puupehenol (**109**) from *Hyrtios digitatus*.[78–81]

2.1.4. *Dasyscyphin*-type SQs. The sesquiterpenoid moiety is connected to the benzoquinone/quinol *via* a cyclopentane ring in dasyscyphin-type SQs. Bioactivity-guided fractionation of the fungus *Stictidaceae* afforded dasyscyphins C, F, and G (**110–112**), and the fourth ring in **110** was corrected to 2-cyclohexene-1,4-dione instead of 2-cyclohexene-1,2-dione upon reference to the typical ^{13}C chemical shift of 1,4-dione, analyzing the HMBC correlations between H-14 and C-13, C-15, C-16, and C-22, and ECD calculations.[82,83] 19-*O*-methylpelorol (**113**) and akadisulfate A (**114**) were purified from the sponges of *Dactylospongia* sp. and *Aka coralliphaga*, respectively.[56,84]

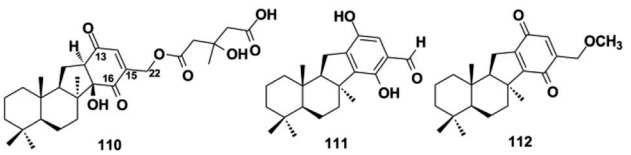

2.1.5. Hymenopsin-type SQs. Hymenopsins A and B (**115–116**) were the first reported secondary metabolites isolated from *Hymenopsis* fungus, which possess a hexatomic and carbocyclic C-ring.[47] Two other analogs, neopetrosiquinones A and B (**117–118**), were discovered in the sponge of *Neopetrosia* cf. *proxima*.[85]

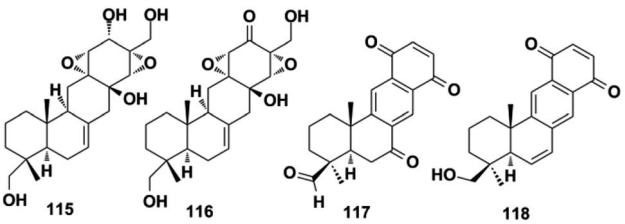

2.2. Avarane-type SQs

The sesquiterpenoid part of avarane-type SQs possess a rearranged drimane scaffold, which are also known as the 4,9-friedodrimane-type, in which one methyl of drimane migrates from the C-4 to C-5 position and the other methyl migrates from the C-10 to the C-9 position. The earliest and most well-known examples of this skeleton type are avarol and avarone, which were isolated from *Dysidea avara*.[3] Avarane-type SQs exist as metabolites, which are only derived from sponges, such as *Dysidea* sp., *Dactylospongia* sp., *Spongia* sp., Smenospongia sp., and *Hyrtios* sp. The H. W. Lin's group have intensively studied the chemical constitution of the above sponges and reported 124 new SQs since the year of 2012, accounting for ~80% of all avarane-type SQs reported to date.[33–37,79,84,86–99] Among these compounds, eight were new skeletons, namely, "Dysiarenone," "Septosone," "Frondoplysin," "Dysideanone," "Spiroetherane," and "Dysidavarone," and rated as "hot off the press" by Natural Product Reports.[33–37,97,100–104]

2.2.1. Typical avarane-type SQs. The sesquiterpenoid and quinone/quinol connect to each other through the C-1′–C-15 bond in typical avarane-type SQs. The *cis* fusion of rings A/B was deduced from the coupling constant of H-10 (J = 6–7 Hz) and the chemical shift of CH_3-12 (δ_C = 32–34 ppm). When rings A/B are in the *trans* position, the coupling constant of H-10 becomes much larger (J = 10–13 Hz) and the ^{13}C NMR chemical shift of CH_3-12 moves significantly upfield to δ_C = 20–21 ppm (Table 1).

Using a hemisynthetic phishing probe coupled with MS/MS molecular networking, dactylocyanines A–H (**119–126**), which possesses an unexpected zwitterionic diamino-*meta*-quinonoid blue scaffold, have been isolated from *Dactylospongia metachromia*.[24] Fucci2 is a newly-developed fluorescent cell cycle probe; a fluorescent image-based high-content screening

Table 1 Representative ^{1}H and ^{13}C NMR data for typical avarane-type SQs with *cis* or *trans*-fused A/B ring

Comp.	$\delta_{H\text{-}10}$ (J in Hz)	$\delta_{C\text{-}12}$	Comp.	$\delta_{H\text{-}10}$ (J in Hz)	$\delta_{C\text{-}12}$
144 [a]	1.09 (br d 6.3)	32.5	202[b]	0.78 (dd 11.6, 1.8)	20.5
145 [a]	1.10 (br d 6.3)	32.5	203[b]	1.04 (m)	19.9
146 [a]	1.11 (br d 6.3)	32.5	204[b]	1.03 (m)	19.8
147 [a]	1.11 (br d 5.9)	32.5	208[b]	0.93 (dd 12.8, 2.3)	20.6
148 [a]	1.11 (br d 6.2)	32.5	209[b]	1.25 (m)	21.6
149 [a]	1.32 (br d 5.7)	32.4	210[b]	1.21 (m)	21.3
200 [a]	1.19 (br d 5.8)	33.5	213[b]	0.78 (dd 12.0, 2.0)	20.8
229 [a]	1.40 (d 6.6)	33.2	217[b]	0.92 (d 13.0)	20.6
231 [a]	1.17 (d 6.0)	33.3	218[b]	0.92 (dd 9.5, 1.5)	20.6
232 [a]	1.19 (m)	33.4	220[b]	0.78 (dd 11.5, 2.0)	20.6

[a] *Cis*-fused A/B ring. [b] *Trans*-fused A/B ring.

technique using HeLa/Fucci2 cells was developed to explore cell cycle inhibitors from *Dactylospongia metachromia*, and three new compounds, namely, neoisosmenospongine (**127**), nakijiquinone I (**128**), and (−)-dictyoceratin-C (**129**), were discovered.[21] More compounds were obtained from *Dactylospongia* sp., which were described as dactylospongins A–D (**130–133**), *ent*-melemeleone B (**134**), melemeleones C–D (**135–136**), dysidaminone N (**137**), nakijinol B (**138**), smenospongines B–C (**139–140**), 19-methoxy-dictyoceratin A (**141**), 5,8-di-*epi*-ilimaquinone (**142**), nakijiquinone V (**143**), 5-*epi*-nakijiquinones S, Q, T, U, and N (**144–148**), and 5-*epi*-nakijinols C–D (**149–150**).[16,84,98,105–107] In addition to *Dactylospongia* sp., *Dysidea* sp. has been found to be an important source of avarane-type SQ metabolites. LC-MS–guided fractionation of *Dysidea frondosa* produced a pair of bioconjugates, frondoplysin A and B (**151–152**), which are composed of a sesquiterpene quinone and an unusual psammaplysin alkaloid.[97] Seventeen structural analogs, dysidaminones A–M (**153–165**) and 19-methyl and 18-, 19-, and 18-phenethyl-substituted aminoavarones (**166–169**) were isolated from the sponge *Dysidea fragilis*.[93] The same research group has also reported cinerols A–K (**170–180**) from *Dysidea cinerea*, 8-ethoxyneoavarone (**181**), 19-ethoxyneoavarone (**182**), 18-ethoxyavarone (**183**), 19-ethoxyavarone (**184**), and (−)-*N*-methylmelemeleone A (**185**) from *Dysidea avara*, dysicigyhone A (**186**) from *Dysidea septosa*, and the first examples of terpene-polyketide-pyridine hybrid metabolites, dysivillosins A–D (**187–190**) from *Dysidea villosa*.[87,88,94,95,108] *Dysidea* sp. sponges have also yielded (+)-19-methylaminoavarone (**191**), 20-methoxyneoavarone (**192**), 17-*O*-acetylavarol (**193**), 17-*O*-acetylneoavarol (**194**), 18-aminoarenarone (**195**), 19-aminoarenarone (**196**), 18-methylaminoarenarone (**197**), 19-methylaminoarenarone (**198**), smenospongimine (**199**), and melemeleones C and D (**200–201**).[55,109–112] We noticed that compounds **200** and **201** were both reported as new

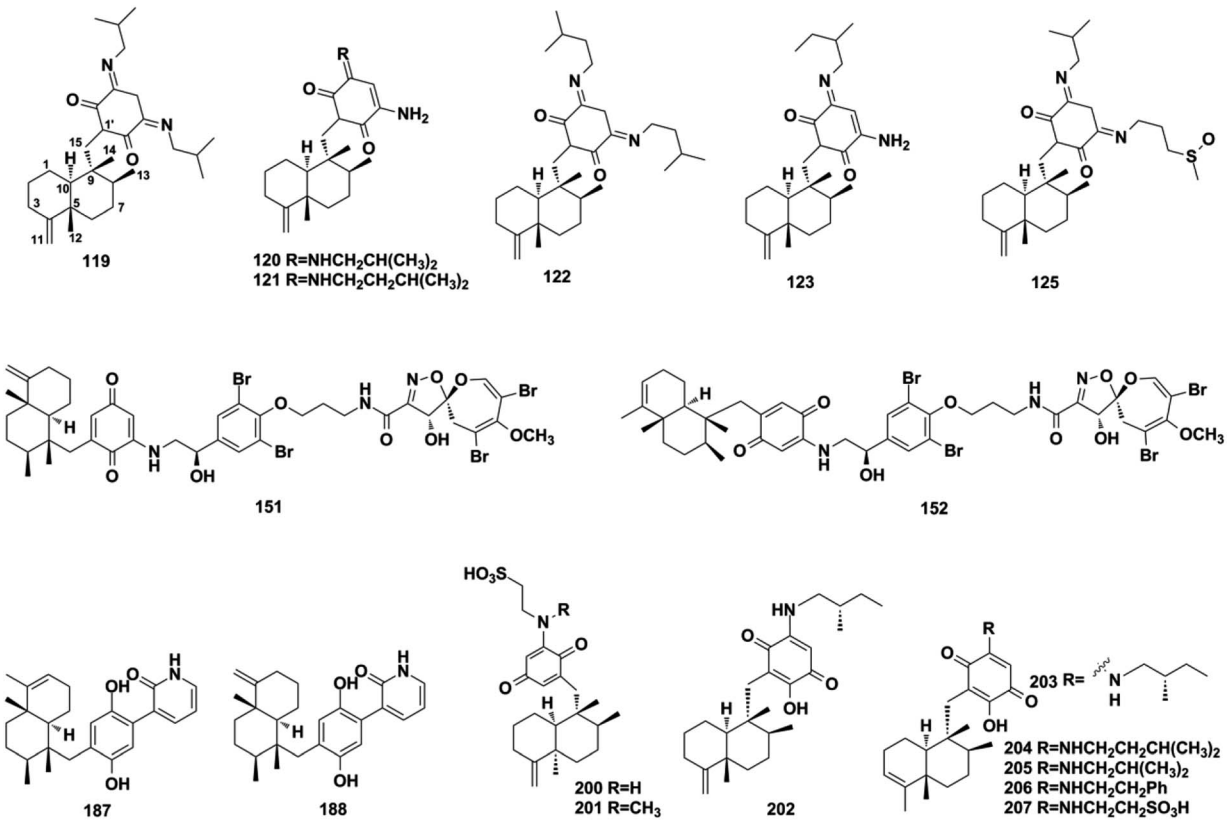

compounds; however, they are isomers of the reported compounds in terms of the stereogenic centers at C-5, C-8, C-9, and C-10, and the double bond positions in the sesquiterpenoid part.[84,109] Nakijiquinones L, K, N, O, Q, and R (**202–207**) were discovered from collections of Okinawan marine sponges of the family *Spongiidae*, and they possess unique side chains derived from amino acids.[113] The chromatographic fractionation of the extract from *Spongia* sp. furnished langconols A–C (**208–210**), langcoquinones A–F (**211–216**), 18-deoxy-18-formamidodictyoceratin B (**217**), 18-deoxy-18-(2-hydroxyacetyl) aminodictyoceratin B (**218**), dictyoceratin D (**219**), *N*-methyl-*ent*-smenospongine (**220**), and *N*-methyl-5-*epi*-smenospongine (**221**).[79,114–116] The chemical investigation of sponges *Hyrtios* sp., *Smenospongia cerebriformis*, and *Aka coralliphaga*, afforded nakijinols F and G (**222–223**), smenohaimiens C–E (**224–226**), and akadisulfate B (**227**), respectively.[56,96,117] Biotransformation has been employed to identify drug leads from the oxidative incubation mixture of *Smenospongia aurea*, *S. cerebriformis*, and *Verongula rigida*, followed by the identification of the structurally new nakijinol E (**228**), 5-*epi*-nakijinol E (**229**), nakijinone A (**230**), 5-*epi*-nakijinone A (**231**), and 5-*epi*-20-*O*-ethylsmenoquinone (**232**).[19]

2.2.2. Dactyloquinone-type SQs. Dactyloquinone-type SQs possess a unique cyclic ether moiety, in which the avarane moiety is tethered to the quinol/quinone *via* a pyran or oxepane ring. The first dactyloquinone-type SQs were discovered in the sponge of *Dactylospongia elegans*.[118,119] Three more congeners have been identified from the same sponge: 8-*epi*-dactyloquinone B (**233**), 20-demethoxy-20-isopentylaminodactyloquinone D (**234**), and 20-demethoxy-20-isobutylaminodactyloquinone D (**235**).[16,98] The chemical exploration of three *Dysidea* sp. collected from China, Federated States of Micronesia, and Japan has afforded dysiquinols A–D (**236–239**), aureol B (**240**), and avapyran (**241**), respectively.[87,109,111] Five new derivatives, namely, 20-demethoxy-20-methylaminodactyloquinone D (**242**), 20-demethoxy-20-methylamino-5-*epi*-dactyloquinone D (**243**), 20-demethoxy-20-ethoxydactyloquinone E (**244**), 20-demethoxy-20-ethoxydactyloquinone B (**245**), and 20-demethoxy-20-methylaminodactyloquinone B (**246**), have been isolated from *Spongia pertusa* Esper and their absolute configurations assigned upon comparing the experimental and calculated ECD spectra and specific optical rotation values with those of known compounds, and biogenetic relationship analysis.[79] The purification of *Smenospongia cerebriformis* yielded smenohaimien F (**247**).[120]

2.2.3. Dysideanone-type SQs. Dysideanone-type SQs possess the 6/6/5/6, 6/6/6/6 fused tetracyclic ring system, featuring the two-point connection between the quinone and sesquiterpene moieties.[35] Dysideanone-type dysiherbols A–C (**248–250**), dysifragilones A–C (**251–253**), dysideanones A–C and E (**254–257**), cycloaurenones A–C (**258–260**), and melemeleone E (**261**) have been reported from *Dysidea* sp. and *Dactylospongia* sp.[35,84,90,92,109] Five years later, the constitution and absolute configuration of **248** was revised by chemical total syntheses, applying two different strategies.[121,122]

2.2.4. Spiroetherane-type SQs. The screening of the anti-angiogenic activity of *Dysidea etheria* using a zebrafish model coupled with LC-DAD/MS chemical profiling analysis has resulted in the discovery of spiroetherones A and B (**262–263**), which have a unique spiro[4,5]decane skeleton.[34] This unprecedented skeleton was named "spiroetherane" and has been proposed to be originated from avarone *via* an intramolecular Michael addition reaction between C-1 and C-16 (Scheme 2). The absolute configurations of compounds **262** and **263** were established as 1*S*,5*S*,8*S*,9*R*,10*S*,16*S* using spectroscopic analysis coupled with quantum chemistry DFT GIAO

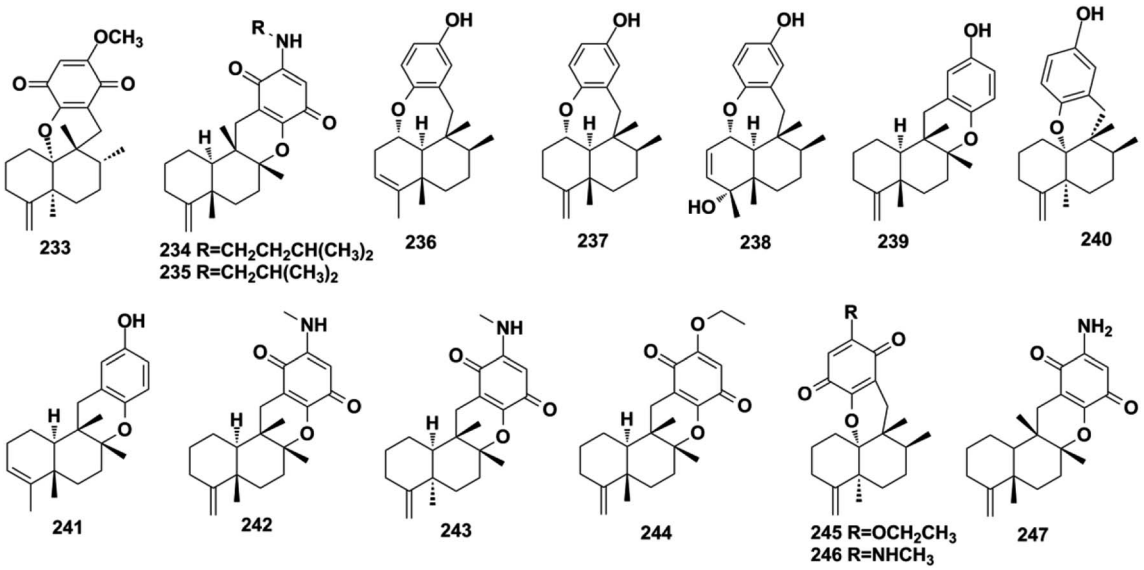

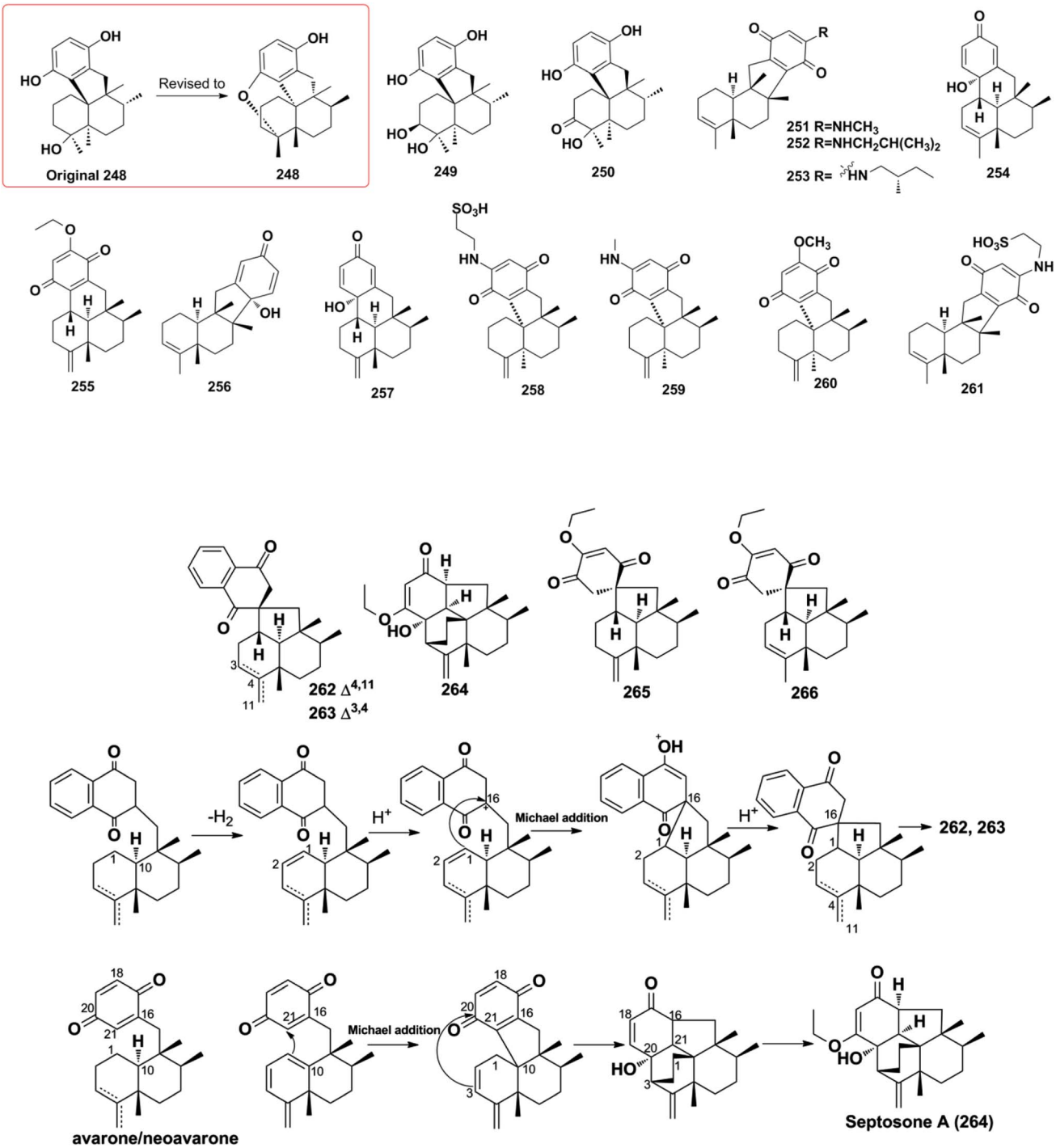

Scheme 1 The proposed biosynthetic pathway for spiroetherones A and B (**262–263**) and septosone (**264**).

^{13}C NMR spectroscopy and ECD calculations. The anti-inflammatory activity screening of *Dysidea septosa* afforded two more spiroetherane-type constituents, septosones B and C (**265–266**), together with septosone A (**264**).[36] The structure of **264** features a characteristic pentacyclo[6.6.2.1^{3,14}0^{1,10}0^{2,7}] heptadecane ring system, which may be derived from avarone/neoavarone *via* a Michael addition reaction between C-10 and C-21, followed by nucleophilic attack from C-3 to C-20 (Scheme 1).

2.2.5. Dysidavarane-type SQs. The novel "dysidavarane" carbon skeleton possesses a unique bicyclo[3,3,1]-nonane carbocycle. Cytotoxicity-guided fractionation of *Dysidea avara*

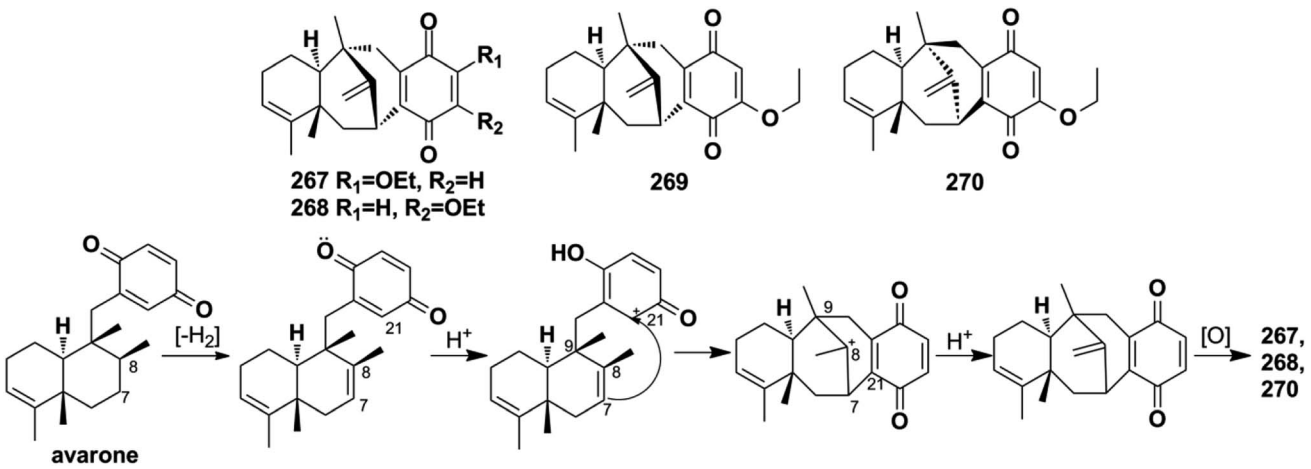

Scheme 2 The proposed biosynthetic pathway of dysidavarones A, B, and D (**267**, **268**, and **270**).

yielded dysidavarones A–D (**267–270**).[33] These compounds have been suggested to be biosynthesized from the common existing avarone, and the key bicyclo[3,3,1]-nonane was constructed *via* an intramolecular nucleophilic addition reaction between C-7 and C-21 (Scheme 2).

2.3. Aureane-type SQs

Aureane-type SQs are the methyl (5 → 4)-abeo products of avarane-type SQs, which feature a *gem*-dimethyl at the C-4 position. The rare iodo-substituted 6′-iodoaureol (**271**) was isolated from the sponge *Smenospongia* sp.[123] Bioassay-guided isolation of the active extract of *Dactylospongia elegans* resulted in 4,5-di-*epi*-dactylospongiaquinone (**272**) and 10,17-*O*-cyclo-4,5-di-*epi*-dactylospongiaquinone (**273**), both with a cyclopropyl ring system characterized by two doublet signals observed at $\delta_H < 1$ ppm, $J = 4.0$ Hz for CH_2-12.[16] Nakijiquinone J (**274**) with (*S*)-2-methylbutylamine and nakijiquinones M and P (**275**, **276**) isolated from the sponges of the *Spongiidae* family exist as amine forms.[113] Myrothecisins C and D (**277–278**) are isolated from the medical plant-derived fungus *Myrothecium* sp. OUCMDZ-2784.[70] Yahazunol B (**279**) is the chemical constituent of *Spongia pertusa* Esper.[79]

2.4. Farnesane-type SQs

Farnesane-type SQs are characterized by a farnesane-type sesquiterpenoid long-chain attached to the quinol unit. A total of 35 papers have described 122 new farnesane-type SQs isolated from the marine sponge *Aka coralliphagum*, the medicinal plant *Rhododendron anthopogonoides*, and five genera of fungi, including *Ganoderma*, *Stachybotrys*, *Penicillium*, *Albatrellus*, and *Alternaria*. Almost all of the metabolites from the *Stachybotrys* species share a common isoindolinone motif. There is a fascinating stereochemical anomaly in which most of the SQs isolated from *Ganoderma* species are found to be enantiomers or racemates, which may be due to the flexibility of the aliphatic chain, and γ-lactones or cyclic ethers are usually formed in these species.

Ganoderma fungi contain more than 80 species, many of which have been used as folk medicine in Asian countries since ancient times. An in-depth investigation has been carried out on *Ganoderma* species by Y. X. Cheng's group and they reported cochlearoids A, B, and E (**280–282**), cochlearoids H–J (**283–285**), (±)-cochlearoids N–Q (**286–289**), cochlearols C, D, R, Q (**290–293**), gancochlearols D, E, and I (**294–296**), and ganomycin K and F (**297–298**) from *Ganoderma cochlear*; lucidumones B–H (**299–305**), dayaolingzhiols C–E (**306–308**), ganodermaone B

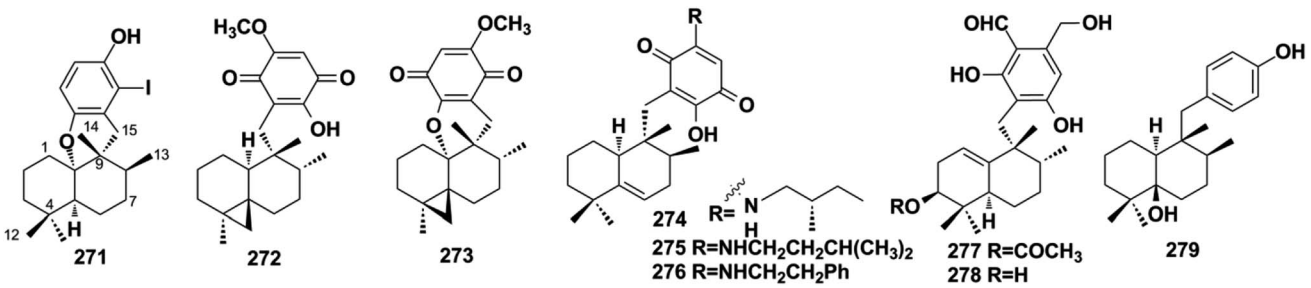

(**309**), and chizhine F (**310**) from *Ganoderma lucidum*; and (±)-zizhines A–F (**311–316**) from *Ganoderma sinensis*.[124–135] Compounds **280–282** and **286–289** possess a unique methanobenzo[*c*]oxocino[2,3,4-*ij*]-isochromene scaffold.[125,126,128] The stereogenic centers of **292** were assigned as 1′*S*, 2′*S*, and 3′*S* using a combination of MAD, $\Delta\delta_{max}$, and R^2 analysis of its ^{1}H NMR chemical shifts in $CHCl_3$, DMSO, and MeOH, and the NMR calculation method was proven to be an effective tool for determining the absolute configuration of compounds that lack efficient ROESY data.[130,131,136] The first stereochemical establishment of compound **297** was assigned as 1*R*,10*S* using the $Rh_2(OCOCF_3)_4$-induced ECD method according to the bulkiness rule.[127] There are also many other studies focusing on the constituents of *Ganoderma* sp., such as ganomycin C (**317**), cochlearins B–E and I (**318–322**) from *G. cochlear*, ganofuran B (**323**) from *G. lucidum*, ganoduriporols C–L (**324–333**) from *Ganoderma ahmadii*, and ganoresinains A, B, and E (**334–336**) from *G. resinaceum*, among which the unique oxepane was formed in the structures of compounds **331–333**.[137–142] Serial fractionation and purification of the marine fungi *Stachybotrys chartarum* and *Stachybotrys longispora* has led to the identification of isoindolinone chartarutines A–H (**337–344**), stachybotrysams A–D (**345–348**), stachybotrin G (**349**), and FGFC2 4–7 (**350–354**), and orsellinic acid-based stachybonoids A–C (**355–357**).[25,26,61,65,143,144] It is worth mentioning that stachybotrin G reported as compounds **349** and **84** have totally different structures.[71,143] A total of 27 *Stachybotrys* Microspora Triprenyl Phenols (SMTP) congeners (**358–384**) with characteristic tricyclic γ-lactam, geranylmethyl, and N-linked side chain, along with their precursor pre-SMTP (**385**), have been reported from amine-fed cultures of *Stachybotrys microspore*.[145–148] Verruculide B (**386**) was obtained from ascidian-derived *Penicillium verruculosum*.[76] Diethyl sulfate (DES) mutagenesis is an effective method used to activate the silent pathways and exploit new metabolites of fungi, and chrysomutanin (**387**) was separated from the DES-mutant *Penicillium chrysogenum*.[28] Amyloid-β aggregation inhibition activity-guided fractionation of *Albatrellus yasudae* has afforded scutigeric acid (**388**), albatrelactone methyl ester (**389**), albatrelactone (**390**), 10′,11′-dihydroxygrifolic acid (**391**), 2-hydroxy-1-methoxy neogrifolin (**392**), and 9′-ketogrifolic acid (**393**).[149,150] Bicycloalternarenes A–F (**394–399**), monocycloalternarenes A–D (**400–403**), and tricycloalternarene J (**404**) are produced by the sponge-derived fungus *Alternaria* sp.[151,152] *Rhododendron anthopogonoides* Maxim has been used as a herbal medicine for rheumatoid arthritis and chronic bronchitis, and four enantiomers (±)-anthoponoids E–H (**405–408**) and (±)-daurichromene D (**409**) were isolated from its twigs and leaves by chiral-phase HPLC using *n*-hexane/isopropanol as the eluent.[153] Four sulfated SQs, siphonodictyals E1–E4 (**410–413**), have been isolated from the sponge *Aka coralliphagum* and the proposed biosynthetic pathway showed that the macrocycle in **413** may be derived from **412** *via* an aldol addition reaction.[81]

2.5. Monocyclofarnesane-type SQs

The sesquiterpenoid moiety of monocyclo-farnesane-type SQs may be derived from cyclization and methyl migration of their

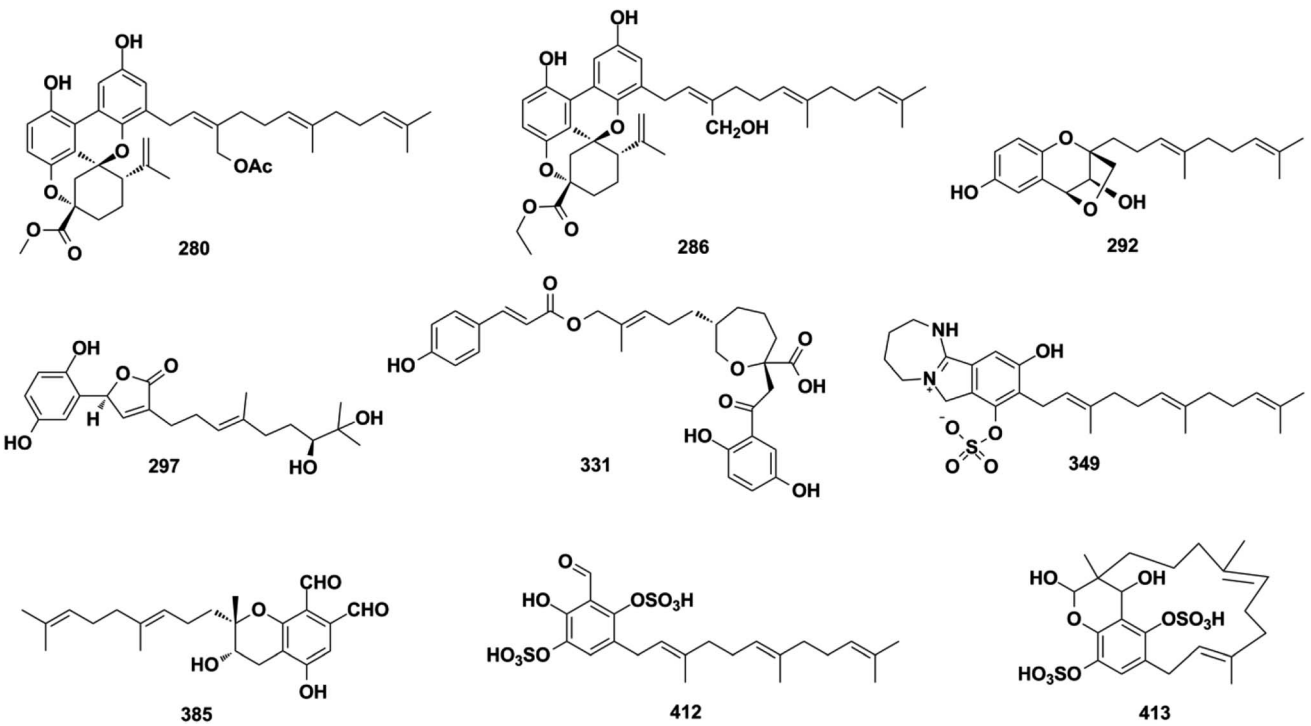

farnesyl precursor. Monocyclofarnesane-type SQs are mainly classified into *cochlioquinone*-type, *metachromiane*-type, *bisabolane*-type, and *tricycloalternarene*-type based on the skeleton of the sesquiterpenoid unit. These compounds are widely distributed in fungi and marine sponges.

2.5.1. *Cochlioquinone*-type SQs. With the rapid development of genome sequencing and bioinformatic analysis technology, genome mining has become a more potent strategy to discover new natural products.[20,22,27] The polyketide synthase, prenyltransferase, and terpenoid cyclase genes have been used to target the mining of two phylo-genetically distinct fungi, *Arthrinium* sp. NF2194 and *Nectria* sp. Z14-w, that led to the isolation of eight cochlioquinone analogs, arthripenoids A–H (**414–421**).[20] The endophytic fungus, *Bipolaris* sp. L1-2, yielded 11 cochlioquinone congeners, bipolahydroquinones A–C (**422**−**424**), cochlioquinones I–N (**425**−**430**), and isocochlioquinones F and G (**431–432**), and their absolute configurations were established using a combination of semi-synthesis, X-ray crystallography analysis, and biosynthetic origin analysis.[154–156] The isolation of phytopathogenic *Bipolaris sorokiniana* and *Bipolaris luttrellii* has afforded 19-dehydroxyl-3-*epi*-arthripenoid A (**433**), 12-keto-cochlioquinone A (**434**), isocochlioquinones D and E (**435–436**), and cochlioquinones F–H (**437–439**).[22,157,158] The above constituents from *Bipolaris* sp., *Arthrinium* sp., and *Nectria* sp. possess a characteristic 6/6/6/6 tetracyclic ring system and 1,3-dimethylpentane substituent. Another endophytic fungus, *Talaromyces purpureogenus*, yielded talaromyolides B, C, and E–K (**440–448**) that bear a 6/6/6/6/6 pentacyclic system.[159,160] The optically pure enantiomers (+)-anthoponoid A (**449**) and (−)-**449** have been purified from the small shrub *Rhododendron anthopogonoides*.[153]

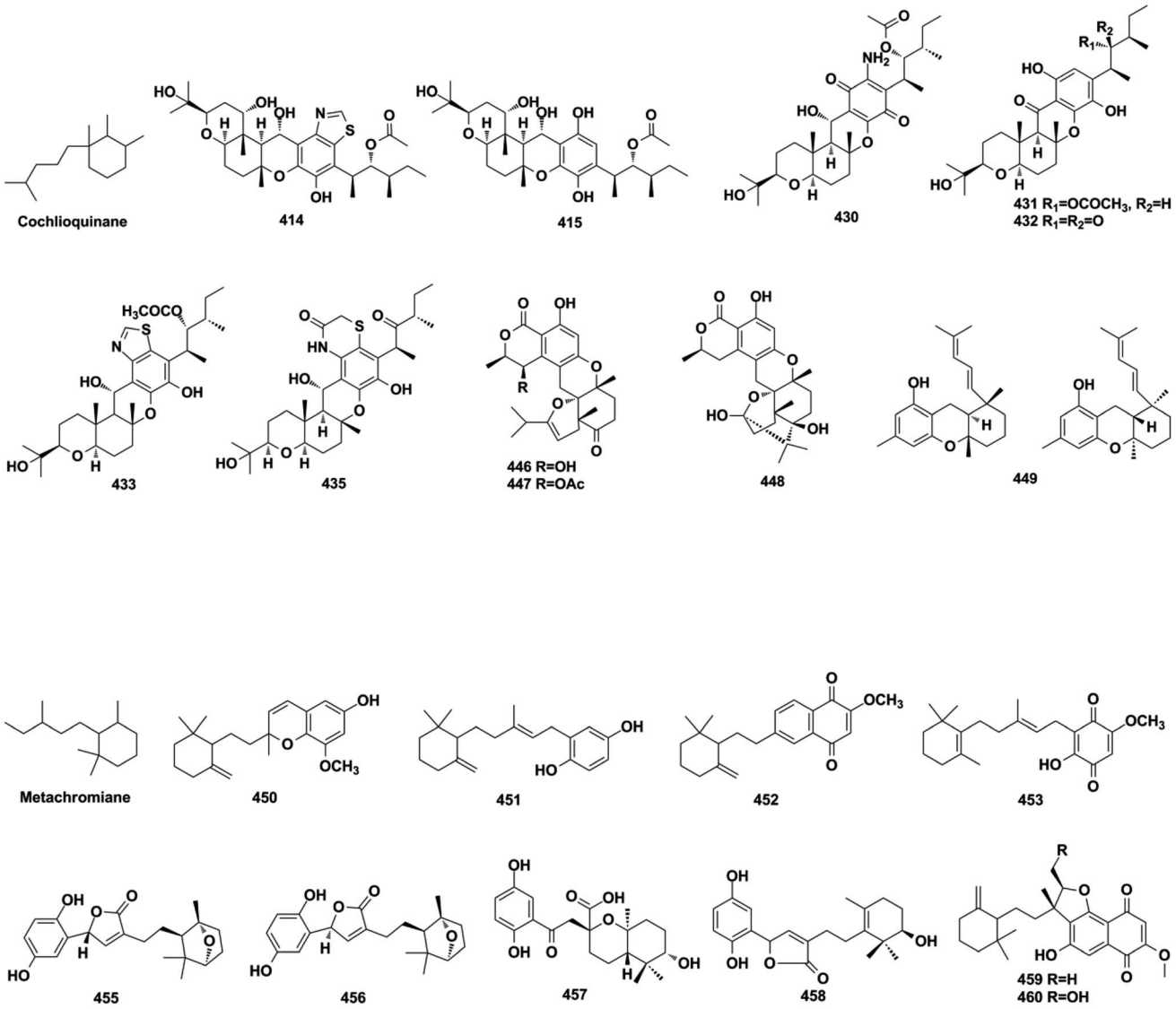

2.5.2. Metachromiane-type SQs. Metachromins U–Y (**450–454**) were purified from the sponges of *Thorecta reticulata* and *Spongia* sp., and the structure of **453** was established using NMR spectroscopy and confirmed by total synthesis employing the brominated monocyclo-farnesane and 1,2,4,5-tetramethoxyzenzene as the starting reagents and using *n*-BuLi/THF-mediated alkylation reaction and $Ce(NH_4)_2(NO_3)_6$ catalyzed oxidization reaction.[161,162] The chemical investigation of *G. cochlear* and *G. resinaceum* has yielded gancochlearols G and H (**455–456**), cochlearol P (**457**), and ganoresinain C (**458**).[127,130,142] The anti-bacterial and cytotoxic extract of the culture media of *Streptomyces niveus* SCSIO 3406 afforded four naphthoquinones, marfuraquinocins A–D (**459–462**).[163]

2.5.3. Bisabolane-type SQs. (±)-Gancochlearols J–N (**463–467**), ganocochlearins A, C, and D (**468–470**), cochlearin A (**471**), cochlearols S, T, U, W, and Y (**472–476**) from *G. cochlea*, and dayaolingzhiols A and B (**477–478**) from *G. lucidum*, are all bisabolane-type SQs.[130,132,136,138,139] The relative structure of gancochlearol L (**465**) was assigned by innovatively applying the NMR calculations and DP4+ probability analysis, then it was purified by chiral HPLC to afford two enantiomers, the absolute configurations of (+)-**465** and (−)-**465**, which were successfully established as 2*S*, 3*R*, 7*R* and 2*R*, 3*S*, 7*R*, respectively, by ECD calculations.[136] The NMR calculation and DP4+ probability method were proved to be an effective way to determine the relative configurations of compounds with ambiguous ROESY data.

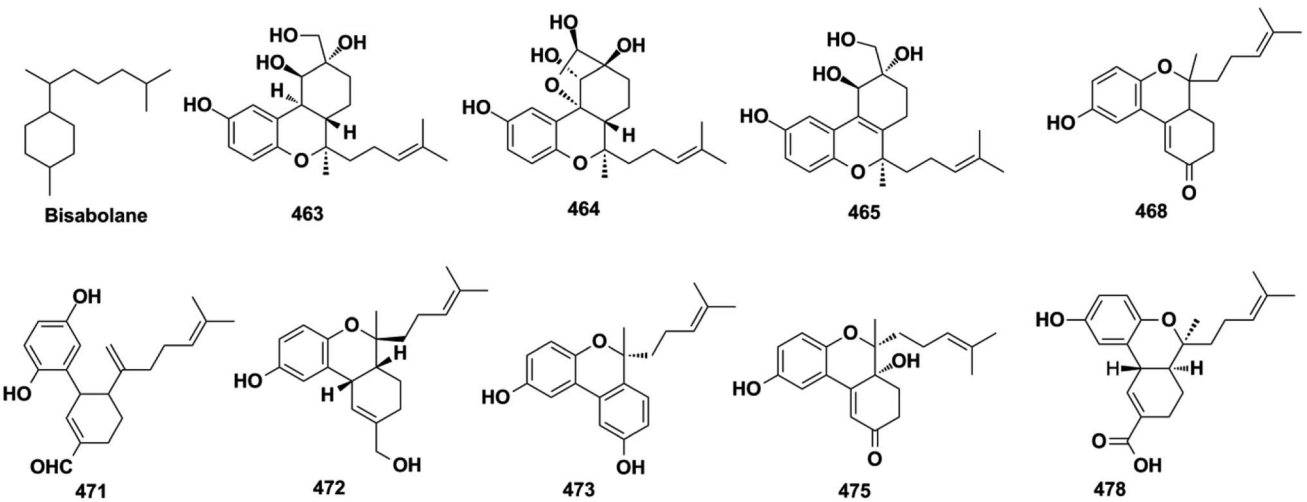

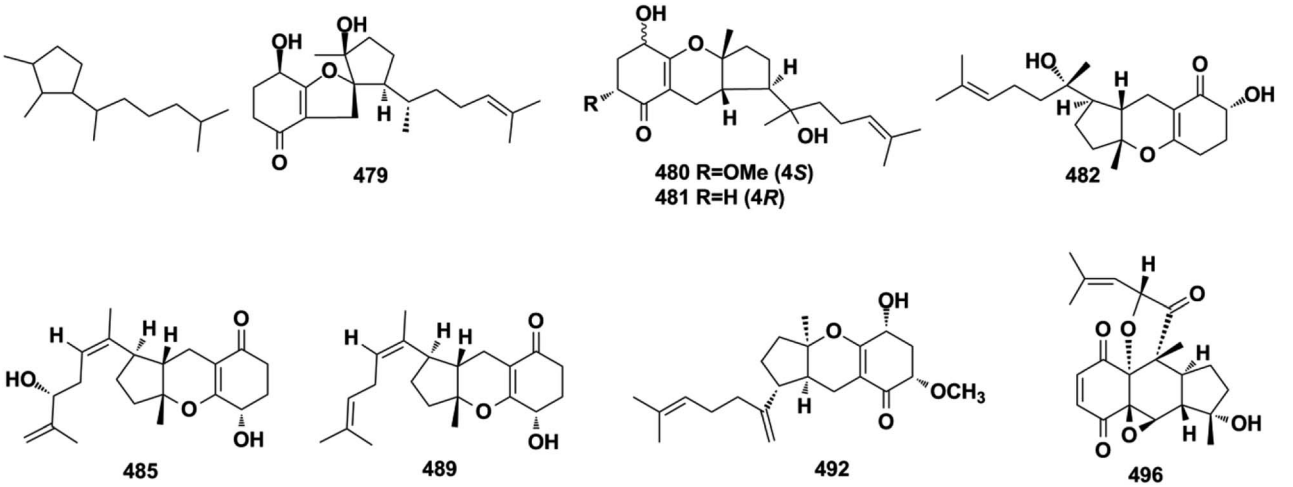

2.5.4. Tricycloalternarene-type SQs. A series of tricycloalternarene analogs have been reported, including tricycloalternarenes A–C, I, and Q–Y (**479–491**) from *Alternaria* sp., guignarenones A and B (**492–493**) from the endophytic *Guignardia bidwellii* PSU-G11, and **479** possesses a unique oxaspiro[5.5]nonane-fused cyclohexanone.[151,152,164–166] The visceral part of ascidian *Aplidium fuegiense* yielded 2,3-epoxyrossinone B (**494**), 3-*epi*-rossinone B (**495**), and 5,6-epoxyrossinone B (**496**), in which the sesquiterpenoid and quinone were connected through two carbon bonds.[167,168]

2.6. Miscellaneous SQs

Miscellaneous SQs usually have rearranged sesquiterpenoid skeletons. Cochlearols B, N, and O (**497–499**), ganodermaone A (**500**), and ganoresinain D (**501**) have been isolated from *G. cochlea* and *G. resinaceum*.[130,133,142,169] Compound **500** has a rearranged carbon backbone that may be derived from fornicin C, which was also purified from *Ganoderma* sp. *via* nucleophilic addition, Wagner–Meerwein rearrangement, cyclization, and esterification (Scheme 3).[133] The sesquiterpenoid moiety of 3-(hept-3^6-enyloxy)-decahydro-4,6*a*,12*a*,12*b*-tetramethyl-1*H*-benzo[*a*]xanthene-4,10,12-triol (**502**), 1-butoxy-4,4,11*b*,11*c*-tetramethyl-decahydrobenzo[*kl*]xanthen-10-ol (**503**) from the macroalga *Gracilaria salicornia*, and peyssonoic acid B (**504**) from the macroalga *Peyssonnelia* sp. feature a rearranged drimane skeleton, and the rearrangement may be catalyzed by *S*-adenosyl methionine-mediated methyl transfer reactions.[51,52] Talaromyolide D (**505**) from *Talaromyces* sp. CX11 has been proposed to originate from 6-hydroxymellein *via* cytochrome P450-mediated epoxidation, epoxide ring

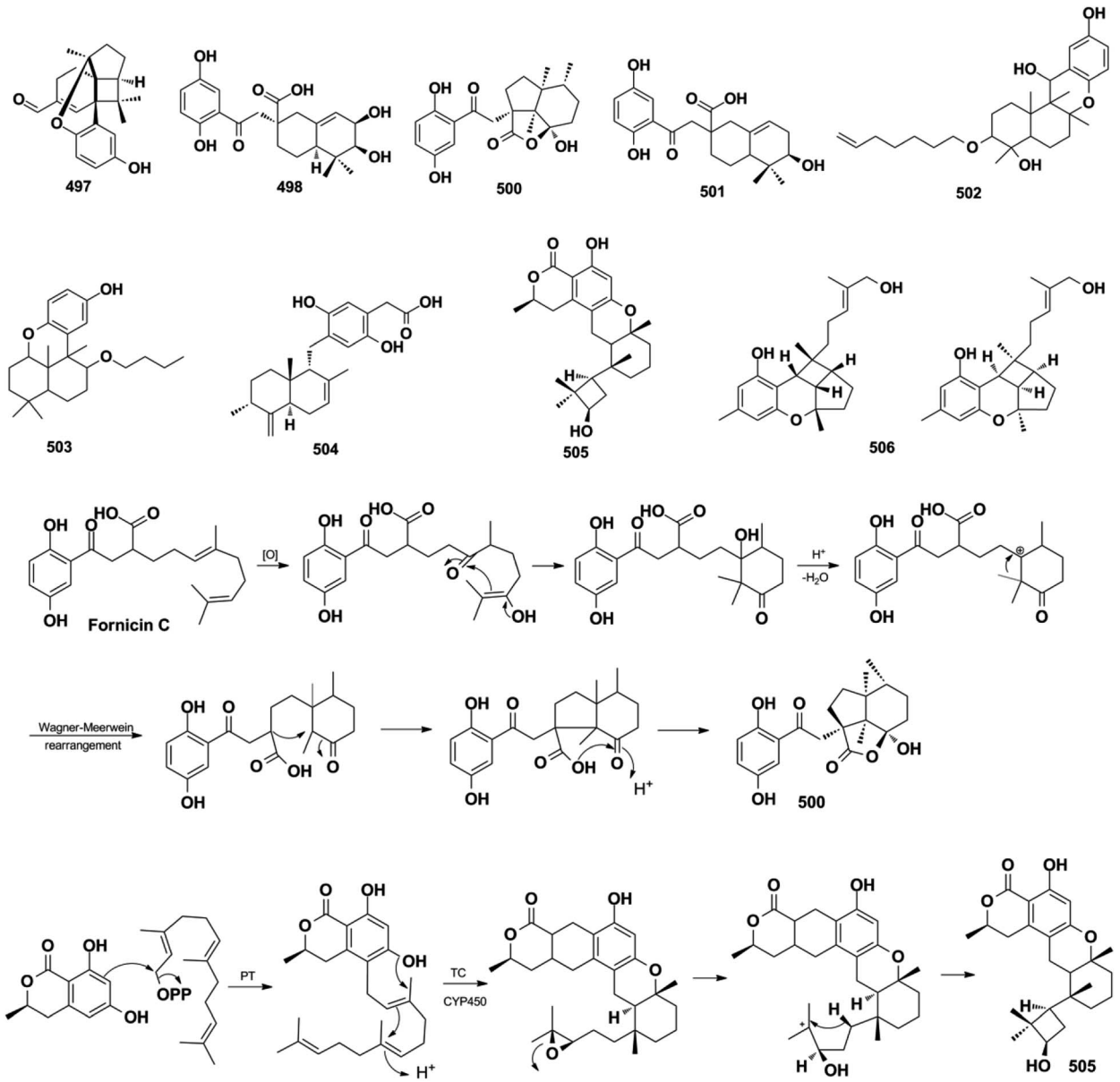

Scheme 3 The proposed biosynthetic pathway of ganodermaone A (**500**) and talaromyolide D (**505**).

opening, and cation intermediate deprotonation (Scheme 3).[159] Optically pure (±)-anthoponoids B–D (**506**–**508**), (±)-fastinoids A and B (**509**–**510**), and (±)-rubiginosin A (**511**) have been isolated from *Rhododendron anthopogonoides* using chiral HPLC.[153,170]

2.7. SQ dimers

SQ dimers are classified into true and pseudo-types according to the dimerization patterns of the two monomers.[171–173] Their molecular weights are in the range of 630–900, which is twice that of their corresponding monomers. In true SQ-dimers, two units of SQs are directly connected *via* one or two C–C bonds. In the pseudo-type, the monomers are linked by ether, amine, or alkyl amine bridges. These SQ dimers are mainly distributed in the fungi of *Stachybotrys* sp. and are widely found in the sponges of the genera *Dysidea*, *Dactylospongia*, and *Smenospongia*. Most of these monomers are phenylspirodrimane-type SQs.

2.7.1. True-SQ dimers. The LC-MS-guided isolation of *Dysidea* sp. led to the discovery of diplopuupehenone (**512**) and dysiarenone (**513**).[37,174] In compound **513**, the central quinone unit is rearranged into a unique 2-oxaspiro[bicyclo[3.3.1]nonane-9,1′-cyclopentane] scaffold, which was proposed to be

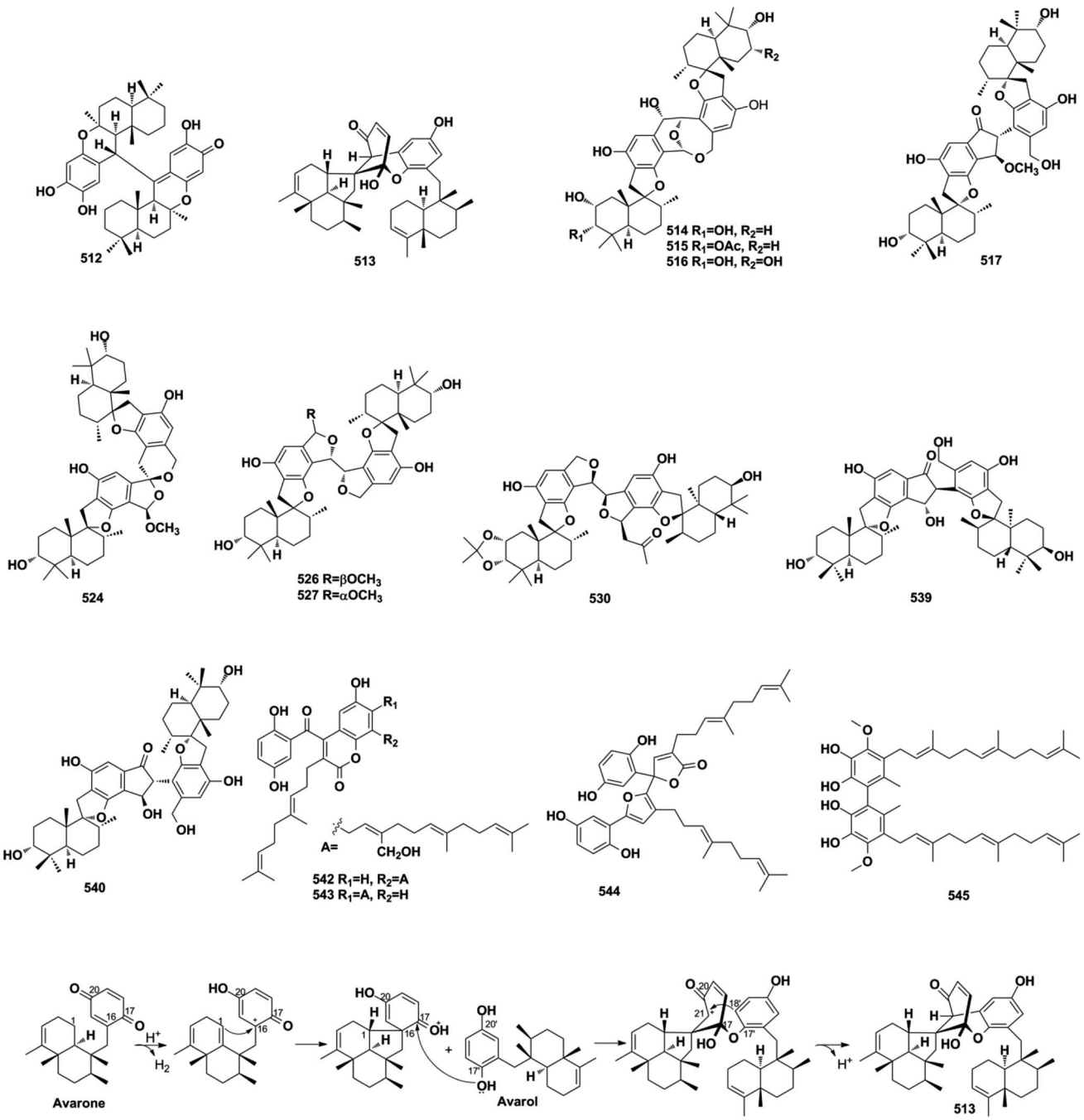

Scheme 4 The proposed biosynthetic pathway of dysiarenone (**513**).

derived from avarone and avarol *via* an intramolecular nucleophilic addition from C-1 to C-16, quinone rearrangement and etherization between C-17 and C-17′, and intramolecular condensation between C-21 and C-18′ (Scheme 4). Bistachybotrysins A–J and L–V (**514–534**) from *S. chartarum* CGMCC 3.5365, stachybochartins A–D (**535–538**) from endophytic *S. chartarum* PT2-12, stachartarin A (**539**), and stachartone A (**540**) from tin mine tailings derived *S. chartarum*, chartarlactam L (**541**), and their corresponding precursor, chartarlactam A, from sponge-derived *S. chartarum* have all been identified as SQ dimers.[63,67,175–180] Among these compounds, **514–516** possess an unusual 2,10-dioxabicyclo[4,3,1]decan-7-ol linkage core, **517–523** and **537–540** are characterized by a central cyclopentanone linkage, and the monomers of **524** and **525** are connected with each other *via* a unique [5,6]-spiroketal core, indicating the diversity of the dimerization patterns formed between the phenylspirodrimane-type SQ monomers.[175–178] The farnesane-type SQ dimers cochlearoids F and G (**542–543**) and gancochlearol C (**544**) are found in the Chinese folk medicine *G. cochlear*.[128,131] Another farnesane-type SQ dimer, bis-2-hydroxy-1-methoxy neogrifolin (**545**), has been isolated from the fungus *Albatrellus yasudae*.[149]

2.7.2. Pseudo-SQ dimers. Chemical investigations on the culture broth of the marine microorganism *Stachybotrys* sp. have yielded unusual stachyin B (**546**) and chartarlactams Q–T (**547–550**), which couple the spirodihydrobenzofuranlactam unit and spirodihydroisobenzofuran unit *via* an N–C connection, and stachybocins E and F (**551–552**) and FGFC1 (**553**) feature an alkylamine linkage.[59,64,181,182] Dimeric popolohuanones G–I (**554–556**) have been obtained from the marine sponge *Dactylospongia elegans*.[86] Popolohuanone F (**557**) together with its precursor, 19-aminoarenarone, has been obtained from the sponge *Dysidea* sp.[112] The third sponge, *Smenospongia* sp., yielded 6′-aureoxyaureol (**558**).[123]

3. Biological activities and mechanisms of action

The natural products provide numerous medicines for disease treatment since ancient times and the natural sesquiterpenod quinone/quinols (SQs) are proved to be important in the new drug discovery process. A fascinating example is avarol that was developed as a topical ointment for psoriasis. It acts by down-regulating the inflammatory cytokines of TNF-α, NF-κB, as well as eicosanoid and superoxide in psoriatic skin.[183,184] It also inhibits the growth of erythroleukemia cells by inducing single-strand breaks of DNA.[6] In addition, avarol exerts potent anti-HIV activities by inhibiting reverse transcriptase and augmenting immune responses proteins selectively.[4,5] However, the anti-HIV studies of avarol by the University Medicine of the Johannes Gutenberg-University Mainz was terminated in clinical phase II. Avarone is the oxidative derivative of avarol, which exhibits 70% curative ratio against leukemia mice at 10 mg kg^{-1} and increases their life span by 146% when the treatment began at day 1, being a promising anti-cancer drug candidate.[185] We may obtain SQs with potential druggability by structural optimization in the far future. The structural diversity of SQs contributes to their broad range of bioactivities. Approximately 48% of all SQ metabolites display potential bioactivity, such as anti-cancer compounds, mainly from *Stachybotrys* sp. and *Dysidea* sp., anti-inflammatory compounds mostly distributed in *Dysidea* sp., anti-microbial components mainly found in fungi, anti-oxidant compounds mainly isolated from *Ganoderma cochlea*, anti-viral metabolites purified from *Stachybotrys* sp. and *Talaromyces* sp., reno-protective metabolites reported from *Ganoderma* sp., and fribrinolytic products discovered from *Stachybotrys* sp.

3.1. Anti-cancer activity

More than one-third of active SQs exhibit anti-cancer activity, providing a rich source of anti-cancer agents (Table 2). They exert anti-tumor activity *via* cytotoxicity, inducing cancer cell apoptosis, cell cycle arrest, preventing migration, inhibiting tumor-associated protein kinases, and blocking angiogenesis. Smenospongine from the sponge *Spongia pertusa* has been identified as a promising candidate agent for breast cancer treatment because significant anti-tumor effects have been observed in mouse xenograft tumor models. It downregulates stem cell markers Nanog, Sox2, and Bmil, induces DNA damage, initiates caspase-dependent apoptosis, and arrests the G0/G1 phase of breast cancer cells MCF7-Nanog *via* the p38/AMPKα pathway.[91] The SQ dimers bistachybotrysins A–B, D–E, M (**514–**

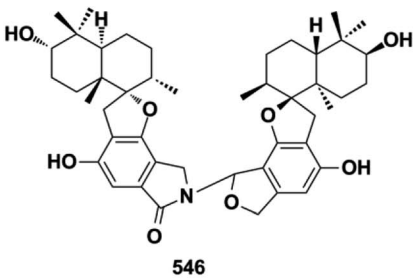

546

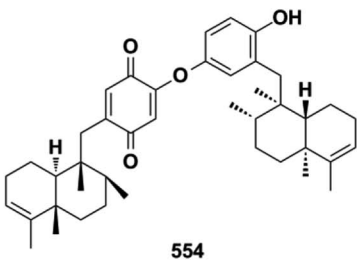

554

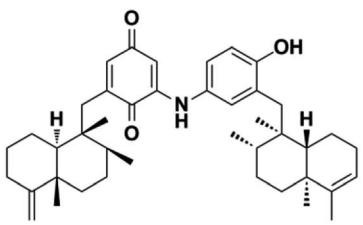

556

Table 2 Anti-cancer activities of representative natural sesquiterpene quinone/quinols

Comp./pos.	IC_{50}	Cells	Ref.
Epoxyphomalin D (**22**)	IC_{50} = 0.72–13.52 μM	T24, BXF 1218L, CNXF 498NL, SF268, HCT116, HT29, GXF 251L, HNXF 536L, LXFL 1121L, LXFA 526L, LXFL 529L, LXFA 629L, H460, MAXF 401NL, MCF-7, MEXF 276L, MEXF 394NL, MEXF 462NL, MEXF 514L, MEXF 520L, OVXF 1619L, OVXF 899L, OVCAR3, PAXF 1657L, PANC1, 22RV1, DU145, PC3M, PXF 1752L, RXF 1781L, RXF 393NL, RXF 486L, RXF 944L, UXF 11138L	49
Chartarolide A (**34**)	IC_{50} = 1.3–5.5 μM	HCT-116, HepG2, BGC-823, NCI-H1650, A2780, MCF-7	62
	IC_{50} = 2.6–9.1 μM	FGFR3, IGF1R, PDGFRb, TrKB	
Chartarolide B (**35**)	IC_{50} = 1.6–4.8 μM	HCT-116, HepG2, BGC-823, NCI-H1650, A2780, MCF-7	
	IC_{50} = 4.9–11.3 μM	FGFR3, IGF1R, TrKB	
Chartarolide C (**36**)	IC_{50} = 5.4–12.5 μM	HCT-116, HepG2, BGC-823, NCI-H1650, A2780, MCF-7	
Taxol[a]	IC_{50} = 0.001–0.09 μM		
Satratoxin H[a]	IC_{50} < 0.5 μM	FGFR3, IGF1R, PDGFRb, TrKB	
Phomoarcherin B (**104**)	IC_{50} = 0.1–9.4 μg mL^{-1}	KKU-100, KKU-M139, KKU-M156, KKU-M214, KB	77
Ellipticine[a]	IC_{50} = 0.19–7.11 μg mL^{-1}		
Dasyscyphin F (**111**)	IC_{50} = 4.1–8.2 μM	MDA-MB-231, MDA-MB-435	83
Taxol[a]	IC_{50} = 0.002–0.007 μM		
19-*O*-methylpelorol (**113**)	IC_{50} = 9.2 μM	PC-9	84
Smenospongine B (**139**)	GI_{50} = 6.0–10.0 μM	SF-268, MCF-7, H460, HT-29	106
	GI_{50} = 3.0 μM	CHO-K1 (normal cells)	
5-*Epi*-nakijiquinone N (**148**)	IC_{50} = 0.97–3.03 μM	ALK, FAK, IGF1-R, SRC, VEGF-R2	105
	IC_{50} = 1.8 μM	L5178Y	
5-*Epi*-nakijinol C (**149**)	IC_{50} = 3.31–7.78 μM	ALK, FAK, IGF1-R, VEGF-R2	
Kahalalide F[a]	IC_{50} = 4.3 μM	L5178Y	
Dysidaminone C (**155**)	IC_{50} = 0.57–8.71 μM	NCI-H929, HepG2, B16F10, SK-OV-3//TNF-α induced HEK293/NF-κB cells	93
	IC_{50} = 0.22 μM		
Dysidaminone E (**157**)	IC_{50} = 0.94–9.52 μM		
	IC_{50} = 0.27 μM		
Dysidaminone H (**160**)	IC_{50} = 0.62–9.65 μM		
	IC_{50} = 0.23 μM		
Dysidaminone J (**162**)	IC_{50} = 0.45–2.89 μM		
	IC_{50} = 0.11 μM		
18-Aminoavarone (**167**)	IC_{50} = 0.68–8.15 μM		
	IC_{50} = 0.05 μM		
5-Fluorouracil[a]	IC_{50} = 0.39–7.64 μM		
Rocaglamide[a]	IC_{50} = 0.12 μM		
Cinerol F (**175**)	IC_{50} = 2.78 ± 0.06 μM	SHP-1	94
(−)-20-Methoxyneoavarone (**192**)	IC_{50} = 0.9–4.6 μM	A549, HeLa, HCT-116, Jurkat, K562, BEL-7402	110
Adriamycin[a]	IC_{50} < 1 μM		
Nakijiquinone L (**202**)	IC_{50} = 4.8–8.9 μM	A549, MCF-7, HeLa/WI-38	115
	IC_{50} = 6.9 μM		
Langconol C (**210**)	IC_{50} = 5.0–7.8 μM		
	IC_{50} = 8.7 μM		
Langcoquinone A (**211**)	IC_{50} = 7.9–9.9 μM		
	IC_{50} = 8.4 μM		
Langcoquinone B (**212**)	IC_{50} = 6.2–8.7 μM		
	IC_{50} = 8.8 μM		
Langcoquinone C (**213**)	IC_{50} = 6.6–9.6 μM		
	IC_{50} = 8.2 μM		
5-FU[a]	IC_{50} = 4.7–5.6 μM		
	IC_{50} = 6.8 μM		
Langcoquinone D (**214**)	IC_{50} = 5.9–8.9 μM	A549, MCF-7, HeLa/WI-38	116
	IC_{50} = 5.6 μM		
5-Fu[a]	IC_{50} = 5.5–6.5 μM		
	IC_{50} = 5.6 μM		

Table 2 (*Contd.*)

Comp./pos.	IC_{50}	Cells	Ref.
(+)-5-*Epi*-20-*O*-ethylsmenoquinone (**232**)	$IC_{50} = 3.24$ μM $IC_{50} = 2.95$ μM	SW480 HCT116	19
Dysiquinol D (**239**)	$IC_{50} = 2.81 \pm 0.01$ μM	NCI-H929	87
Rocaglamide[a]	$IC_{50} = 3.94 \pm 0.02$ μM		
Aureol B (**240**)	$IC_{50} = 4.8$–5.9 μM	K562, A549	109
DOX[a]	$IC_{50} = 0.8$–1.6 μM		
20-Demethoxy-20-methylaminodactyloquinone D (**242**)	$K_d = 4.8$ μM	CDK-2	79
Dysiherbol A (**248**)	$IC_{50} = 0.58 \pm 0.02$ μM	NCI-H929	92
Avarol[a]	$IC_{50} = 3.32 \pm 0.1$ μM		
Rocaglamide[a]	$IC_{50} = 3.9 \pm 0.1$ μM		
Spiroetherone A (**262**)	$IC_{50} = 2.4 \pm 0.3$ μM $IC_{50} = 7.4$–12.2 μM	Zebrafish model NCI-H929, A549, HepG2, SK-OV-3	34
Spiroetherone B (**263**)	$IC_{50} = 8.7 \pm 0.6$ μM	Zebrafish model	34
(−)-Cochlearoid N (**286**)	$IC_{50} = 7.68$ μM	K562	126
(+)-Cochlearoid P (**288**)	$IC_{50} = 6.63$ μM		
Taxol[a]	$IC_{50} = 0.0023$ μM		
Metachromin V (**451**)	$GI_{50} = 3.2$–10.0 μM $GI_{50} = 2.1$ μM	SF-268, MCF-7, H460, HT-29/CHO-K1 (normal cells)	162
Paclitaxel[a]	$GI_{50} = 0.01$–0.02 μM $GI_{50} = 5.9$ μM		
Staurosporine[a]	$GI_{50} = 0.04$–11.0 μM $GI_{50} = 0.13$ μM		
Bistachybotrysin A (**514**)	$IC_{50} = 2.8$–7.5 μM	HCT116, NCI-H460, Daoy	177
Bistachybotrysin B (**515**)	$IC_{50} = 4.2$–6.6 μM	NCI-H460, BGC823, Daoy	
Bistachybotrysin D (**517**)	$IC_{50} = 6.8$–7.5 μM	HCT116, HepG2	178
Bistachybotrysin E (**518**)	$IC_{50} = 6.7$–8.9 μM	HCT116, BGC823	
Bistachybotrysin M (**525**)	$IC_{50} = 1.8$–3.5 μM	HCT116, NCI-H460, BGC823, Daoy, HepG2	175
Taxol[a]	$IC_{50} = 0.0002$–0.01 μM	HCT116, NCI-H460, BGC823, Daoy, HepG2	175, 177 and 178
Paclitaxel[a]	$IC_{50} = 0.002$–0.038 μM		
Stachybochartin C (**537**)	$IC_{50} = 11.6 \pm 1.6$ μM $IC_{50} = 14.5 \pm 3.1$ μM	MDA-MB-231/U2-OS	67
Stachybochartin D (**538**)	$IC_{50} = 10.4 \pm 0.9$ μM $IC_{50} = 9.2 \pm 0.1$ μM		
Cisplatin[a]	$IC_{50} = 11.3 \pm 0.6$ μM $IC_{50} = 5.9 \pm 1.3$ μM		
Doxorubicin[a]	$IC_{50} = 1.0 \pm 0.1$ μM $IC_{50} = 1.2 \pm 0.9$ μM		

[a] Positive control

515, **517–518**, **525**) from *S. chartarum* are cytotoxic on HCT116, NCI-H460, BGC823, Daoy, and HepG2 cells with IC_{50} of 1.8–8.9 μM.[175,177,178] Epoxyphomalin D (**22**) displays highly potent cytotoxicity by inhibiting the proliferation of 34 types of cancer cells, including liver cancer, melanoma, ovarian cancer, and renal cancer cells with IC_{50} values in the range of 0.72–13.52 μM.[49] The overgrowth of angiogenesis from an existing vascular system is usually found in solid tumors, and preventing angiogenesis is an important anti-cancer approach. Spiroetherones A and B (**262–263**) from *Dysidea etheria* inhibit the angiogenesis of zebrafish with IC_{50} values of 2.4 ± 0.3 and 8.7 ± 0.6 μM, respectively; compound **262** is also cytotoxic toward NCI-H929, A549, HepG2, and SK-OV-3 cancer cells with IC_{50} values in the range of 7.4–12.2 μM, exhibiting a combined anti-cancer mechanism.[34] Chartarolides A and B (**34–35**) and 5-*epi*-nakijiquinone N (**148**) inhibit the proliferation of HCT-116, HepG2, BGC-823, NCI-H1625, A2780, MCF-7, and L5178Y cancer cell lines with IC_{50} values in the range of 1.3–5.5 μM, which may be mechanistically related to the inhibition of a group of cancer-related kinases, including FGFR3, IGF1R, PDGFRb, TrKB, ALK, FAK, IGF1-R, SRC, and VEGF-R2 (IC_{50} = 0.97–11.3 μM).[62,105] While 5-*epi*-nakijinol C (**149**), cinerol F (**175**), and 20-demethoxy-20-methylaminodactyloquinone D (**242**) only inhibit tumor-related kinases of ALK, FAK, IGF1-R, VEGF-R2, SHP-1, and CDK-2 with IC_{50} values at 2.78–7.78 μM.[79,94,105] Metastasis occurs when cancer spreads from the primary location to secondary sites and is the major driving force of cancer patient mortality. (−)-Lucidumone B (**299**), (−)-lucidumone D (**301**), (+)-lucidumone F (**303**), and (+)-lucidumone H (**305**) selectively inhibit Kyse30 cell migration at a nontoxic

concentration of 20 μM and their anti-metastatic effects are related to the downregulation of *N*-cadherin.[135] Gancochlearol I (**296**) suppresses the epithelial–mesenchymal transition of triple-negative breast cancer cells (MDA-MB-231) by down-regulating the key factors of TWIST1 and SNAI1 at 20 μM, providing valuable drug candidates for the treatment of cancer metastasis.[127] Nuclear factor κB (NF-κB) plays a key role in the proliferation, migration, and apoptosis of cancer cells, and is an important target for anti-cancer drug discovery. Dysidaminones C, E, H, and J (**155**, **157**, **160**, and **162**), and 18-aminoavarone (**167**) inhibit NF-κB in HEK293 cells with IC_{50} values in the range of 0.05–0.27 μM, and they are also cytotoxic toward NCI-H929, HepG2, B16F10, and SK-OV-3 cancer cells with IC_{50} values in the range of 0.45–9.65 μM. Structure–activity relationship analysis has shown that the 18-amino group in the quinone unit is essential for cytotoxicity and NF-κB inhibitory activity.[93] The WNT pathway is commonly activated in many cancers and its activation is dependent on β-catenin-related gene transcription. (+)-5-*epi*-20-*O*-ethylsmenoquinone (**232**) inhibits the proliferation of CRT-positive SW480 and HCT116 colon cancer cells *via* the inhibition of Wnt/β-catenin and accelerating cytosolic β-catenin degradation at 1.5–6.0 μM.[19] Stachybochartin C (**537**) time- and dose-dependently inhibits colony formation (0.5–2.0 μM) and proliferation (1.5–50 μM) in U-2OS cells, and the remarkably increased caspase-8, caspase-9, and PARP indicate that this effect was associated with caspase-dependent apoptosis.[67] Many SQs exhibit multiple bioactivities. 19-*O*-methylpelorol (**113**), dysiquinol D (**239**), dysiherbol A (**248**), and gancochlearol I (**296**) display anti-tumor (IC_{50} = 0.58–9.2 μM) and anti-inflammatory activities (IC_{50} = 0.49–9.2 μM).[84,87,92,127] Dasyscyphin C (**110**), langcoquinones C and D (**213–214**), aureol B (**240**), and (+)-cochlearoid P (**288**) exhibit both cytotoxic (IC_{50} = 4.1–9.6 μM) and anti-microbial activities (MIC = 2–8 μg mL^{-1}, 6.25–12.5 μM).[83,109,115,116,126] Phomoarcherin B (**104**) exerted inhibition on five human epidermoid carcinoma and adenocarcinoma cells (IC_{50} = 0.1–9.4 μg mL^{-1}) and antimalarial activity against *P. falciparum* with IC_{50} = 0.79 μg mL^{-1}.[77] Bistachybotrysin M (**525**) prevents HCT116, NCI-H460, BGC823, Daoy, and HepG2 cancer cell proliferation with IC_{50} values in the range of 1.8–3.5 μM, and it also exerts neuroprotective effects toward glutamate-induced toxicity (17.4% at 10 μM) that is comparable to reservatrol (16.1% at 10 μM).[175] Although smenospongine B (**139**), nakijiquinone L (**202**), langconol C (**210**), langcoquinones A–D (**211–214**), and metachromin V (**451**) are cytotoxic toward several cancer cells with IC_{50} or GI_{50} values in the range of 4.8–10.0 μM, the lack of selectivity in normal cell lines (GI_{50} on CHO-K1 = 2.1–3.0 μM, IC_{50} on WI-38 = 5.6–8.8 μM) may make them difficult to develop into new anti-cancer drugs in the future.[106,115,116,162]

3.2. Anti-inflammatory activity

About half of the anti-inflammatory SQs possess avarane-type structure. 19-*O*-methylpelorol (**113**), dactylospongins A–B, D (**130–131**, **133**), *ent*-melemeleone B (**134**), and dysidaminone N (**137**) inhibit the production of inflammatory cytokines IL-6, IL-8, IL-1β, and PEG2 in LPS-induced THP-1 cells with IC_{50} of 5.1–9.2 μM.[84] Dysiherbol A (**248**) inhibits NF-κB production in TNF-α-induced RAW264.7 cells with an IC_{50} value of 0.49 μM, which is 10- and 20-fold more potent than that of dysiherbols B and C (**249–250**), respectively, indicating that the increased degree of oxidation at C-3 dramatically decreases the anti-inflammatory activity.[92] Dysifragilone A (**251**) has comparable anti-inflammatory activity with that of hydrocortisone succinate, which inhibits the enzymatic activity and protein expression of iNOS and COX-2, the release of downstream NO, PGE2, and IL-6 by selectively blocking the p38/MAPK pathway in LPS-stimulated RAW264.7 cells.[90,99] At concentrations of 2.5–10 μM, septosone A (**264**) exhibits anti-inflammatory activity comparable to that of indomethacin in alleviating migration and decreasing the number of macrophages surrounding zebrafish neuromasts.[36] The gancochlearol E (**295**), (+)-gancochlearol I (**296**), (−)-gancochlearol I (**296**), gancochlearol G (**455**), and gancochlearol H (**456**) with γ-valerolactone unit inhibit the COX-2 enzyme with IC_{50} of 1.03–2.02 μM (IC_{50} of $pos._{celecoxib}$ = 0.03 μM), and the inhibitory effect of both enantiomers of **296** shows little difference.[127] The inhibitory effects of (+)-anthoponoid E (**405**), (−)-anthoponoid G (**407**), and anthoponoid H (**408**) on IL-1β and NF-κB support the traditional use of *Rhododendron anthopogonoides* for rheumatoid arthritis.[153] The simultaneous inhibitory effect of COX-2/5-LOX is important for lipoxin synthesis to resolve inflammation. The 3-(hept-3^6-enyloxy)-decahydro-4,6*a*,12*a*,12*b*-tetramethyl-1*H*-benzo[*a*]xanthene-4,10,12-triol (**502**) significantly inhibits COX-2, 5-LOX, and COX-1 with IC_{50} values in the range of 1.33–1.57 mM, and the calculated binding energy of −12.30 kcal mol^{-1} with 5-LOX further substantiates its anti-inflammatory potential.[52] The anti-inflammatory effect of the SQ dimer dysiarenone (**513**) increases 10 times when compared with that of avarol, indicating the importance of the unique 2-oxaspiro[bicyclo[3.3.1]-nonane-9,10-cyclopentane] scaffold. Further mechanism study indicated that **513** dose-dependently inhibited COX-2 enzyme expression and the corresponding PGE2 production in LPS-induced RAW264.7 cells without affecting COX-1 expression at 0–8 μM.[37]

3.3. Anti-microbial activity

Three-quarters of anti-microbial SQs are sensitive to the *Staphylococcus* and *Bacillus* strains. Aureol B (**240**, MIC = 1–8 μg mL^{-1}), with the key quinol functional group being considerably more active than melemeleones C–D (**135–136**), and cycloaurenones A–C (**258–260**) bearing the quinone moiety for inhibiting the growth of bacterial *S. aureus*, *B. subtilis*, *S. enterica*, and *P. hauseri*, and the fungus *T. rubrum*, may be attributed to the high amount of reactive oxygen radicals produced by the quinol unit.[109,186] The SQ dimers stachyin B (**546**) and chartarlactams Q, S (**547**, **549**) inhibit *S. aureus*, methicillin-resistant *S. aureus*, *B. subtilis*, and *S. epidermidis* with IC_{50} of 1.02–1.75 μM and 4–8 μg mL^{-1}, which are comparable to the positive control chloramphenicol (IC_{50} = 1.45–2.46 μM, 1.0 μg mL^{-1}); this may be due to the superior ability of the dimers in binding double sites in the target.[59,181] Both (+)-cochlearoid P (**288**) and (−)-cochlearoid (**288**) inhibit the

growth of *S. aureus* with IC_{50} < 10 μM, while the activity of (+)-cochlearoid O (**287**) (IC_{50} = 17.99 μM) decreased when compared with its enantiomer (−)-cochlearoid O (**287**) (IC_{50} = 6.28 μM), indicating the significant influence of the farnesyl position (IC_{50} of $pos._{ciprofloxacin}$ = 0.21 μM).[126] The typical avarane-type SQs of smenospongimine (**199**), nakijiquinone L (**202**), and langcoquinones A–D (**211–214**) are sensitive to the strains of both *B. subtilis* and *S. aureus* with MIC values of 3.13 μg mL^{-1} or 6.25–25.0 μM (MIC of $pos._{chloromycetin/ampicillin}$ = 3.13 μg mL^{-1}, 6.25–25.0 μM).[55,113–116]

3.4. Anti-diabetic activity

PTP1B is considered a potential target in type II diabetes because of its negative regulatory effect on insulin receptors. Seventeen SQs, including verruculide A (**100**), frondoplysins A and B (**151–152**), cinerols A–C, and F (**170–172**, and **175**), 17-*O*-acetylavarol (**193**), 17-*O*-acetylneoavarol (**194**), nakijinol G (**223**), avapyran (**241**), dysidavarone A (**267**), and ganoduriporols C, D, F, G, and H (**324**, **325**, and **327–329**), exhibit potent anti-diabetic activity by inhibiting PTP1B with IC_{50} values in the range of 0.39–20.0 μM.[33,76,94,96,97,111,137,141] Among these compounds, frondoplysin A–B (**151–152**) display more potent activity than the positive control ($IC_{50/oleanolicacid}$ = 3.7 ± 0.03 μM) in inhibiting PTP1B with IC_{50} of 0.39 ± 0.04 μM and 0.65 ± 0.03 μM, and **151** is proved to be a mixed PTP1B inhibitor by detailed enzymatic kinetic study.[97] Molecular docking showed that ganoduriporol F (**327**) forms H-bonds with ALA-217, GLN-266, and ARG-24, which are located in the active site of PTP1B.[137] In addition, craterellin A (**12**) significantly inhibits the 11β-HSD2 enzyme that regulates the glucose-raising hormone with an IC_{50} value of 1.5 μg mL^{-1}, and myrothecisin C (**277**) inhibits α-glucosidase with an IC_{50} value of 5.8 μM.[44,70]

3.5. Anti-oxidant activity

A transgenic fluorescent zebrafish experiment has shown that frondoplysin A (**151**) exhibits anti-oxidative activity over five times stronger than that of vitamin C at nontoxic concentrations in the range of 10–40 μM.[97] Dysidaminone H (**160**) protects against oxidative injury in HaCaT cells *via* the activation of Nrf2/ARE/HO-1, which is mediated by the phosphorylation of AMPK/ERK at concentrations of 2.5–10 μM.[89] Puupehenol (**107**) has been shown to be a potent anti-oxidant with an FRAP value of 2500 at 1.0 mg mL^{-1} ($pos._{vitaminC}$ 870 at 1.0 mg mL^{-1}).[80] The anti-oxidant activities of 13-[[2-(hexyloxy)-2,5,5,8*a*-tetramethyldecahydro-1-naphthalenyl](methoxy)methyl] benzenol (**29**), akadisulfate B (**227**), ganomycin C (**317**), cochlearins B–E, and I (**318–322**), ganocochlearins A, C, and D (**468–470**), cochlearin A (**471**), 3-(hept-3^6-enyloxy)-decahydro-4,6*a*,12*a*,12*b*-tetramethyl-1*H*-benzo[*a*]xanthene-4,10,12-triol (**502**), 1-butoxy-4,4,11*b*,11*c*-tetramethyl-decahydrobenzo[*kl*]xanthen-10-ol (**503**), and diplopuupehenone (**512**) have been tested using $DPPH^+$, $ABTS^+$, and OH radical scavenging assay, and they show comparable anti-oxidant activities with the positive controls trolox, vitamin C, α-tocopherol, and butylated hydroxytoluene.[52,56,138,139]

3.6. Anti-viral activity

Stachybotrin D (**51**) has been found to be a novel non-nucleoside reverse transcriptase inhibitor of both wild-type HIV-1 and five NNRTI-resistant HIV-1 strains with EC_{50} values in the range of 6.2–23.8 μM (EC_{50} of $pos._{nevirapine}$ = 0.23–51.9 μM).[64] Stachybotrysins A, B, and G (**66**, **67**, and **72**) and stachybotrysams A–C (**345–347**) show inhibitory effects on HIV-1 virus with IC_{50} values in the range of 1.0–19.6 μM (IC_{50} of $pos._{efavirenz}$ = 2.0–4.0 nM).[60,61] Although chartarutines B, G, and H (**338**, **343**, and **344**; IC_{50} = 5.57–5.58 μM) exhibit weaker anti-HIV activity than efavirenz (IC_{50} = 0.65 μM, CC_{50} = 40), their lower cytotoxicity (CC_{50} > 100) suggests that they are worthy of further investigation as anti-HIV candidates.[25] Chartarlactam T (**550**) blocks ZIKU virus replication by targeting the NS5 and E proteins at a concentration of 10 μM.[181] Stachybotrysins A and F (**66** and **71**), and stachybotrysin (**77**) effectively inhibit influenza A virus with IC_{50} values in the range of 12.4–18.7 μM (IC_{50} of $pos._{ribavirion}$ = 2.0–4.0 nM).[60,69] Talaromyolide K (**448**) dose-dependently inhibits pseudorabies virus at concentration in the range of 3.13–50 μg mL^{-1} and prevents pseudorabies virus-causing cell injury with low toxicity to the host cells.[160]

3.7. Fibrinolytic activity

SMTPs metabolites activate the fibrinolytic system by inducing conformational changes in plasminogen, in which the ionizable group in the N-linked side chain is essential for their fibrinolytic activity.[146] As the most representative congener, SMTP-7 has been proven to be a promising thrombolytic candidate for the treatment of ischemic stroke and cerebral infarction in rodents and primates.[187,188] The SMTP dimer FGFC1 (**553**) acts as a promising thrombolytic agent by dose-dependently hydrolyzing fibrin at concentrations in the range of 5–25 μmol L^{-1}, effectively dissolving pulmonary thrombus in the rat lung without risk of hemorrhagic activity at 5–25 mg kg^{-1}.[182,189] FGFC6 and FGFC7 (**353** and **354**) show competitive fibrinolytic activities with relative activities of 6.90 and 3.86 at 0.025 g L^{-1} (pos. 6.46), whereas FGFC4 and FGFC5 were inactive, which may be due to the loss of the carboxyl acid group in the N-linked chain.[26] SMTPs-19, 22, 25, and 43 (**366**, **369**, **372**, and **380**) bearing phenylamine-based side chains are as potent as SMTP-7 (E_{max}/EC_{10} = 1.57-fold μM^{-1}) in enhancing urokinase-catalyzed plasminogen activation (E_{max}/EC_{10} = 1.16–1.57-fold μM^{-1}).[145,147]

3.8. Reno-protective activity

The excessive activation of TGF-β reduces the degradation of extracellular matrix components, which are the hallmarks of renal fibrosis. The overexpression of fibronectin is a common feature of renal disease. Cochlearoids H and I (**283–284**), (+)-cochlearol S (**472**), (−)-cochlearol U (**474**), (+)-cochlearol U (**474**), (−)-cochlearol Y (**476**), and cochlearoids F and G (**542** and **543**) exhibit significant reno-protective activity by inhibiting the viability of TGF-β1-induced NRK-49F cells and fibronectin production in TGF-β1-induced HKC-8 cells at nontoxic concentrations in the range of 2.5–20 μM.[130,131] Cochlearol B

(**497**) inhibits collagen I, fibronectin, and αSMA in TGF-β1-induced NRK-52E cells at concentrations in the range of 5–20 μM, and this action is dependent on the disruption of Smad2 and Smad3 activation.[169] (−)-Gancochlearols J and K (**463** and **464**) and ganodermaone B (**309**) dose-dependently inhibit the viability of TGF-β1-induced NRK-52e cells by attenuating extracellular matrix collagen I and fibronectin at nontoxic concentrations in the range of 10–40 μM.[133,136] MCP-1 is considered to be a new diagnostic marker and therapeutic target for progressive renal injury, chizhine F (**310**) dose-dependently reduces fibronectin and MCP-1 expression in high-glucose-stimulated rat mesangial cells at concentrations in the range of 2.5–10 μM.[134] These reno-protective components from *Ganoderma* fungi provide evidence for their use in kidney disorders.

3.9. Other activities

19-Methoxy-9,15-ene-puupehenol (**109**) exhibits anti-atherosclerosis activity by effectively upregulating SR-B1 (130%) in HepG2 cells at a concentration of 1.78 μM ($pos._{trichostatinA}$ = 5.25 μM, 100%), and it satisfies both Veber's and Lipinski's rule for drug-like molecules with oral bioavailability.[78] Acetylcholinesterase (AChE) inhibitors are the drugs of choice for the treatment of Alzheimer's disease. Dayaolingzhiols D and E (**307–308**) inhibit AChE with IC_{50} values of 8.52 ± 1.90 and 7.37 ± 0.52 μM ($pos._{tacrine}$ = 7.37 ± 0.52 μM), respectively.[132] Scutigeric acid (**388**) and bis-2-hydroxy-1-methoxy neogrifolin (**545**) exhibit anti-Alzheimer's disease activity by inhibiting Aβ aggregation with IC_{50} values of 6.6 and 12.3 μM ($pos._{myricetin}$ = 7.4 and 9.9 μM), respectively, and compound **388** also inhibits β-secretase with an IC_{50} of 1.6 μM ($pos._{myricetin}$ = 2.8 μM).[149,150] Cochlearoid A (**280**) has potent activity toward Cav3.1 TTCC through channel gating modulation (IC_{50} = 11.4 μM, Hill coefficient = 1.6; IC_{50} of $pos._{mibefradil}$ = 10.4 μM, Hill coefficient = 1.6), indicating its possible application in neurological disorders.[125] Arthripenoid C (**416**) possesses immune-suppressive activity by inhibiting ConA-induced T cells and the corresponding production of TNF-α and IFN-γ with an IC_{50} value of 4.2–8.8 μM.[20] Dysivillosins A–D (**187–190**) exhibits anti-allergic activity by inhibiting the release of β-hexosaminidase and downregulating the production of LTB4 and IL-4 in antigen-stimulated RBL-2H3 mast cells at concentrations in the range of 6.0–19.9 μM, and the action of compound **187** was triggered by suppressing the Syk/PLCγ1 pathway.[95] Chartarlactams D–F, K, L, N, and O (**39–41**, **46**, **541**, **48**, and **49**) exhibit potent lipid-lowering effects at 10 μM, as assessed by Oil Red O staining, and compounds **40** and **41** inhibit both intracellular triglyceride and total cholesterol levels in HepG2 cells.[63] Stachybotrysin (**77**) attenuated RANKL-induced osteoclast differentiation by suppressing *c*-Fos, ERK, JNK, and p38 while activating NFATc1 at 5.0 μg mL^{-1}.[69] Gancochlearol C (**544**) inhibits the tuberculosis-related enzyme NAT2 with an IC_{50} value of 5.29 ± 0.1 μM.[128] Chrodrimanins D–F (**89–91**) display insecticidal activity against silkworms with LD_{50} values of 20, 10, and 50 μg g^{-1}, respectively.[73]

4. Total synthesis and biosynthesis

The stereo-controlled synthesis of SQs with attractive structures and exciting bioactivities usually takes many years. Therefore only a few compounds discovered in the recent ten years have been successfully synthesized. For example, avarol and avarone were first discovered in 1974, then they were synthesized by the groups of EA Theodorakis, SM Hecht, AS Sarma, and T Katoh during the years 1982–2008.[190–194] EA theodorakis developed an enantioselective synthesis of avarol and avarone by constructing the entire framework through C11–C1′ bond and using Barton's radical decarboxylation method. In addition, the biosynthetic strategy can also produce scarce natural products, which acts more efficiently by providing a concise cascade reaction. In the process of exploring new biosynthetic methods, new pathways, gene clusters, and the encoded enzyme functions are discovered.[20,27,195,196]

4.1. Total synthesis

4.1.1. Synthesis and structure revision of dysiherbol A. In 2021, H. G. Schmalz's group reported an enantioselective total synthesis of (−) dysiherbol A (**248**) due to its intriguing structure, potent cytotoxic, and NF-κB inhibitory activities.[121] They synthesized optically pure **248** in 12 steps with 5% overall yield. The core tetracyclic skeleton of **248** was built up through the $AuCl_3$-catalyzed twofold cyclization. The C-5-bridgehead methyl was installed in a single step *via* proton-induced *cyclo*-propane opening and cyclic ether formation (Scheme 5). The synthetic structure was secured by the combination of X-ray crystallography, NMR, GC-MS (*m*/*z* 312, 100%), optical rotation, and CD spectra. It has an identical spectroscopic data with the natural product dysiherbol A, except that the optical rotation direction and CD spectra of the two compounds are opposite.[92] Therefore, the synthetic and natural dysiherbol A are supposed to be enantiomers, and the originally proposed structure of dysiherbol A was revised, as depicted in Scheme 5. It is very noticeable that H. W. Lin's group originally assigned the molecular formula of dysiquinol A to be $C_{21}H_{30}O_3$, which has one more water molecule than the correct structure. Coincidentally, the two hydroxyls at C-4 and C-20 undergo a dehydration reaction to generate the correct structure. The dehydration of diols to ether was ignored since it was difficult to recognize in ^1H and ^{13}C NMR data. Therefore, the *m*/*z* of 313.3 should be the $[M + H]^+$ ion peak of the correct structure.[92] The wrong molecular formula leads to the failure of structure elucidation, which may indirectly lead to the incorrect absolute configuration elucidated by ECD calculation. In the same way, the structure of dysiherbol B (**249**) should also be corrected as it has the same optical rotation direction and similar CD spectrum to that of dysiherbol A, and the *m*/*z* of 329.1 should be the $[M + H]^+$ ion peak of the correct structure.[92] The determination of the absolute configuration of natural products is very challenging; even if their relative structure is correct, the ECD calculation technique has an error rate of 4% in absolute configuration determination.[197]

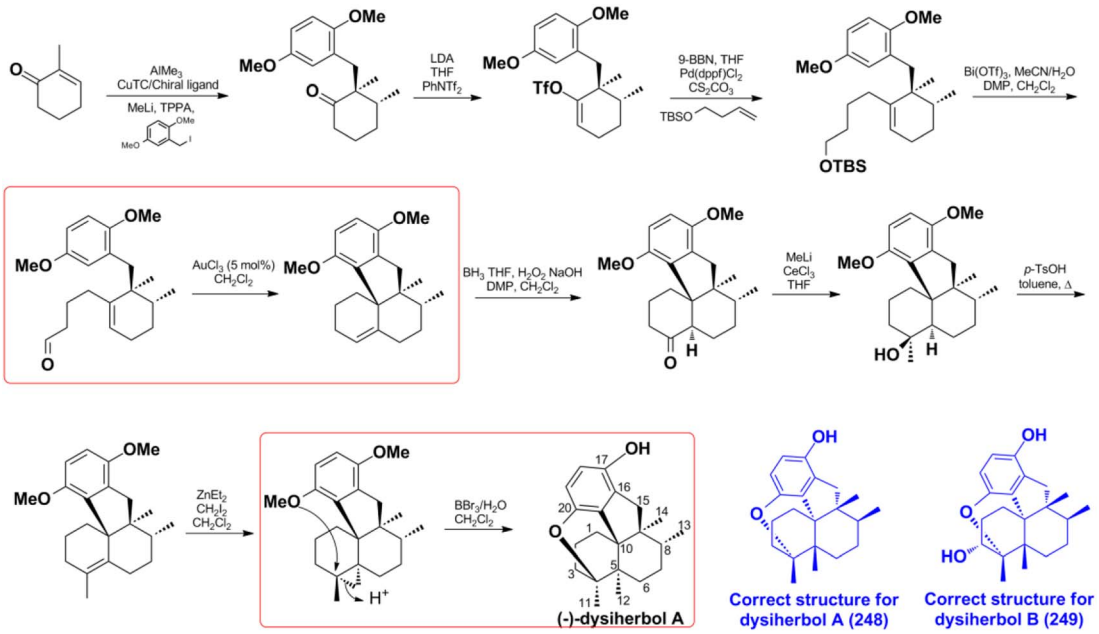

Scheme 5 The total synthesis of dysiherbol A (**248**).

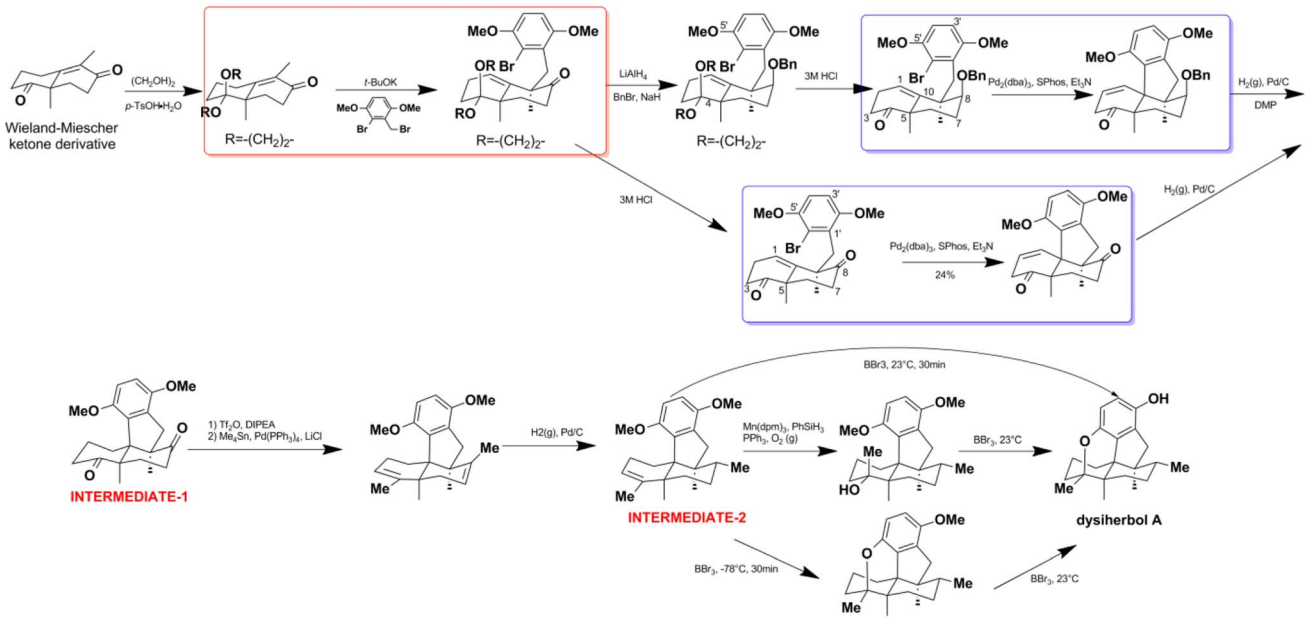

Scheme 6 The total synthesis of dysiherbol A (**248**).

Z. Y. Lu's group disclosed a different synthetic strategy for dysiherbol A (**248**); the compound was obtained in the racemic form, and the revised structure of **248** is the same as that of Schmalz's group (Scheme 6).[121,122] Two of the most important steps are to connect the terpene and quinol moieties stereoselectively using Wieland–Miescher ketone and bulky benzyl bromide, and to construct the 6/6/5/6-fused tetracyclic skeleton using intramolecular Heck reaction. The 6/6/5/6-tetracyclic intermediate-1 can be obtained in the presence of $Pd_2(dba)_3$, SPhos, and Et_3N, irrespective of the presence of axial-OBn or ketone group at the C8 position. However, the glycol acetal on C4 must be removed because the methoxyl on C5′ and the acetal would be very close when the cyclization reaction occurs. Dysiherbol (**248**) comes from intermediate-2 through three different pathways including (1) directly from intermediate-2 using BBr_3 at 23 °C, (2) olefin hydration mediated by $Mn(dpm)_3$, $PhSiH_3$, O_2, and PPh_3, intramolecular etherification, and then demethylation, (3) etherification and then demethylation. Z. Y. Lu and C. K. Chong highlighted the above synthetic method.[198] Echavarren *et al.* constructed the 6/6/5/6 carbocyclic core for

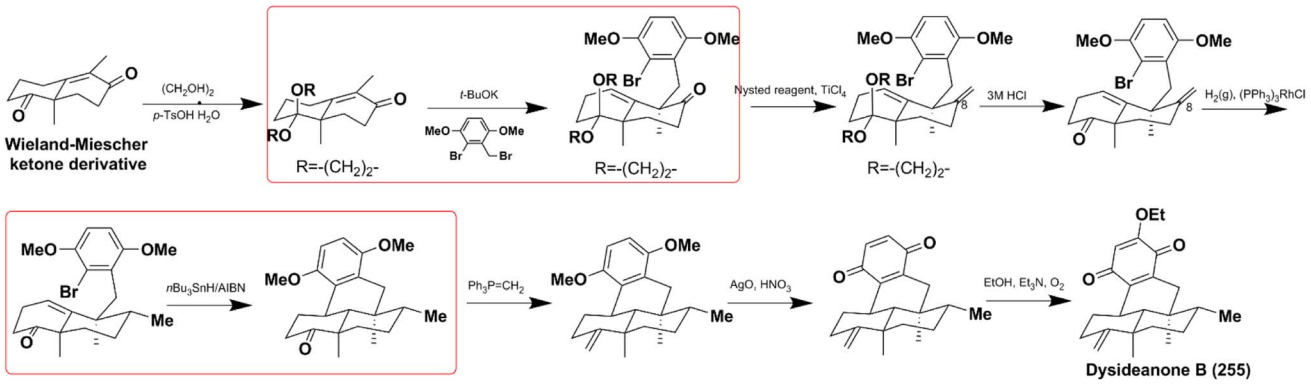

Scheme 7 The total synthesis of dysideanone B (**267**).

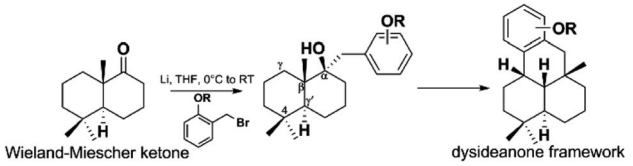

Scheme 8 Construction of the 6/6/6/6 framework of dysideanone.

dysiherbols A–C (**248–250**) *via* gold(I)-promoted (3 + 2) cycloaddition between terminal allenes and dimethoxyphenyl carbenes, and then AIBN-triggered radical cyclization.[199,200]

4.1.2. Synthesis of dysideanone B. Dysideanone B (**255**) possesses unique 6/6/6/6 carbotetracycles and exhibits significant cytotoxicity on HeLa and HepG2 cancer cells. It is synthesized by stereoselective C9-alkylation and nBu$_3$SnH/AIBN-catalyzed intramolecular radical cyclization.[122] Another important process is the methylation of C8-carbonyl, which relies on the Nysted reagent/TiCl$_4$ catalyzed methylenation, and then (PPh$_3$)$_3$RhCl involved diastereoselective reduction (Scheme 7).

Jana *et al.* successfully constructed dysideanone's fused 6/6/6/6 framework by applying the intramolecular γ-arylation of

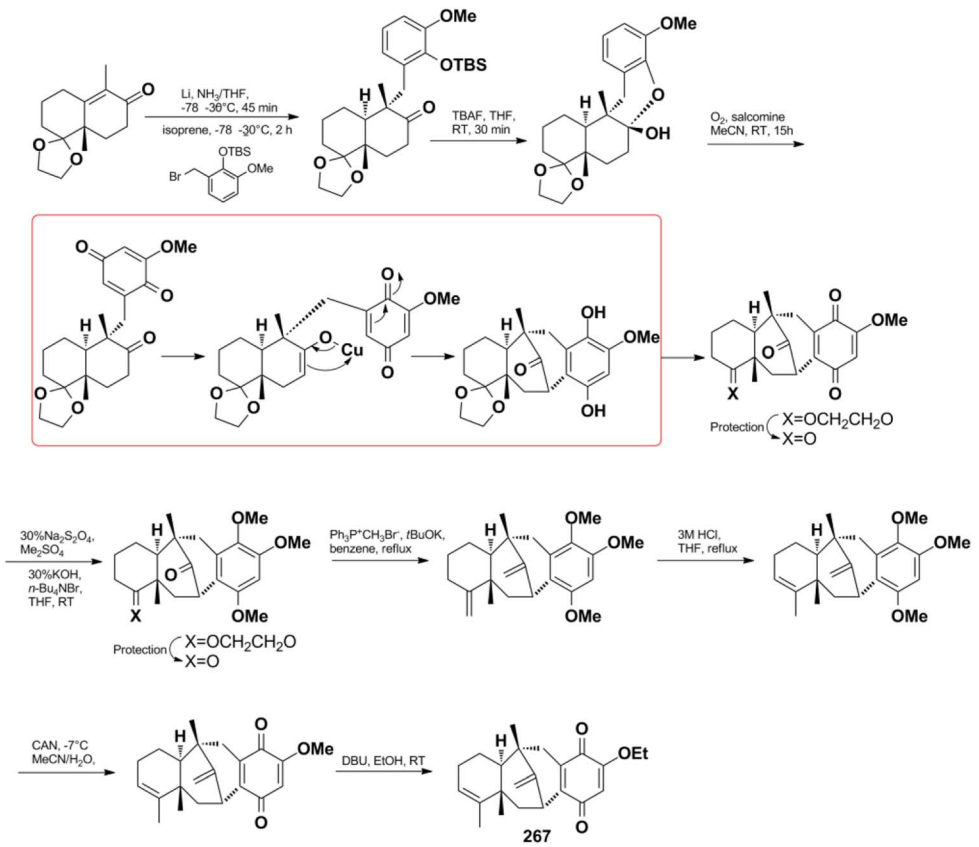

Scheme 9 The total synthesis of dysidavarone A (**267**).

cycloalkanols starting from Wieland–Miescher ketone derivative.[201–203] Computational investigation proved that the regioselective γ-arylation of cycloalkanols are more preferred by 3.4 kcal mol^{-1} when there are two methyl substituents on C-4 (Scheme 8).[204]

4.1.3. Synthesis of dysidavarone A. Dysidavarone A (**267**) possesses an unprecedented "dysidavarane" carbon skeleton, which exhibits significant PTP1B inhibitory, cytotoxicity, and anti-bacterial activity.[33] However, the scarcity of the sample has hindered further pharmaceutical investigations. Inspired by the biosynthetic pathway, Katoh *et al.* successfully synthesized **267** in 13 steps with an overall 30% yield (Scheme 9). The highly strained and bridged eight-membered carbocyclic core was constructed *via* C7–C21 bond formation using a copper enolate-mediated intramolecular Michael addition reaction.[205] The successful synthesis of **267** validated the rationality of the proposed biosynthetic pathway.

Menche *et al.* also successfully synthesized dysidavarone A (**267**) in 10 steps with a total yield of 11% (Scheme 10). They built the core tetracyclic structure *via* the stereoselective reaction of a Wieland–Miescher-type ketone and benzyl bromide, followed by the pivotal $Pd(OAc)_2$ ligand-catalyzed intramolecular ketone α-arylation reaction.[206] The synthetic method confirmed the unique 3D structure of dysidavarone A and provided another concise route for constructing complex fused ring systems of this type of congeners.

4.2. Biosynthesis

4.2.1. Hybrid PKS pathway for arthripenoids A–F. The biosynthetic gene cluster and biosynthetic pathway of arthripenoids are elucidated by gene inactivation, heterologous expression, and biochemical analysis.[20] The quinol moiety is biosynthesized from the highly reducing polyketide synthase/non-reducing polyketide synthase (AtnH/AtnG) pair. It then undergoes AtnJ-mediated oxidative *ipso*-decarboxylation, AtnF-catalyzed farnesyl transfer, AtnA- and AtnK-encoded epoxidation, atnI-initiated terpene cyclization, atnM-induced hydroxylation, atnB-induced keto-reduction, and AntC-mediated acetylation reaction to produce arthripenoid B (**415**). Arthripenoid B (**415**) was easily oxidized to the key intermediate, which then undergoes cysteine addition, followed by ring contraction, tautomerization, H_2O/NH_3 addition, or dehydration to give arthripenoids A, C–F (**414**, **416–419**). This research provided valuable information for the future combinatorial biosynthesis of arthripenoid-type analogs (Scheme 11).

4.2.2. HR-PKS pathway for chrodrimanin-type SQs. Matsuda Y. *et al.* provided a platform for the selective and efficient biosynthesis of chrodrimanin-type SQs under the catalysis of *cdm* gene cluster-encoded enzymes (Scheme 12).[196] The CdmE enzyme with KS-AT-DH-MT-ER-KR-ACP domain architecture is first reported and it synthesizes the nonterpenoid backbone of 6-hydroxymellein without the assistance of other enzymes. 6-Hydroxymellein then generates key 3-hydroxypentacecilide A under the catalysis of prenyltransferase CdmH, epoxidase CdmI, and terpene cyclase CdmG. The key intermediate produces a series of chrodrimanin-type compounds such as chrodrimanins C, E, F, H (**88**, **90**, **91**, **93**) and verruculide A (**100**) in the presence of oxidative tailor enzymes of CdmA, CdmD, CbmJ, and acetyltransferase of CdmC. CdmA, and CdmD are characterized as C-1/C-2 dehydrogenase C-7′ β-hydroxylase, and CdmA acts before CdmD. However, the weak substrate specificities of CdmA, CdmD, and CbmJ lead to multiple pathways to chrodrimanin B, and which pathway mainly occurs needs further investigation.

4.2.3. NR-PKS pathway for funiculolides A–D. The heterologous reconstitution experiments proved that funiculolides A–D (**96–99**) are originated from the 5-methylorsellinic acid (5-MOA) (Scheme 13). 5-MOA is produced under the catalysis of

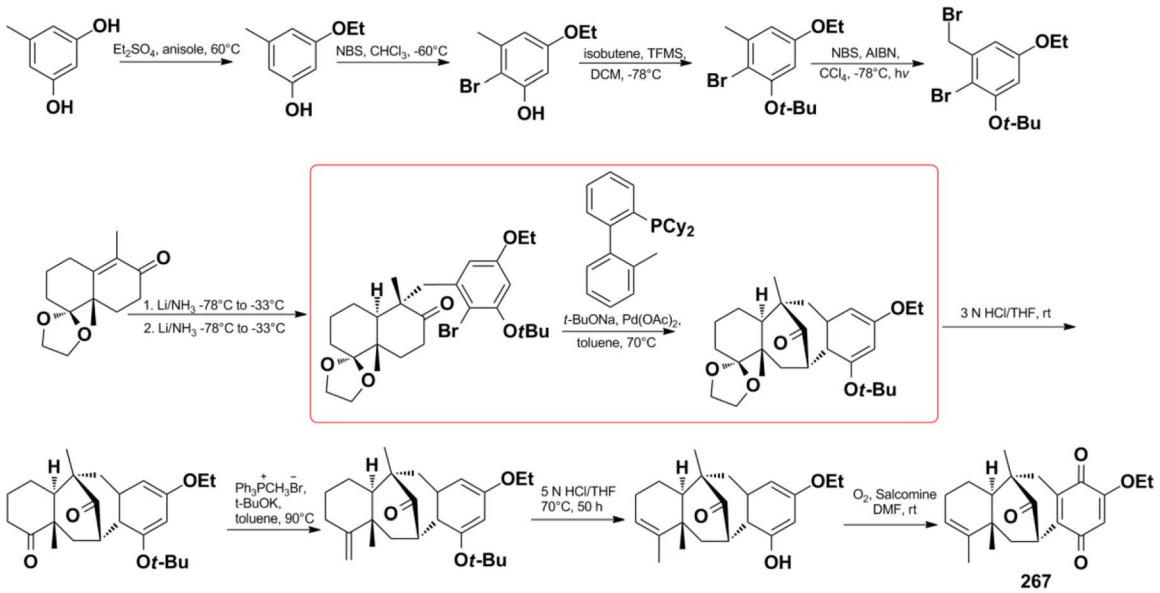

Scheme 10 The total synthesis of dysidavarone A (**267**).

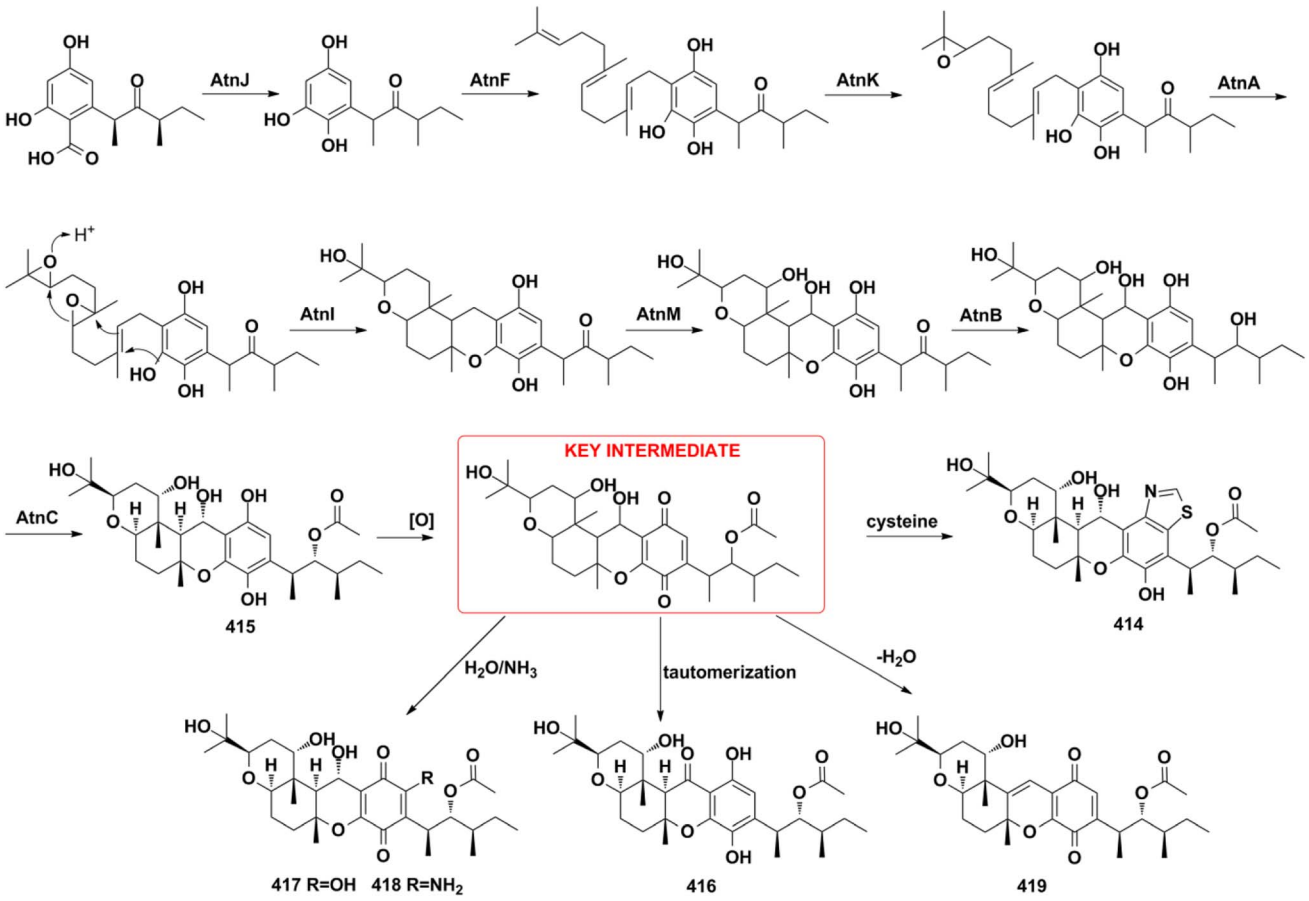

Scheme 11 Biosynthesis of arthripenoids A–F (**414–419**).

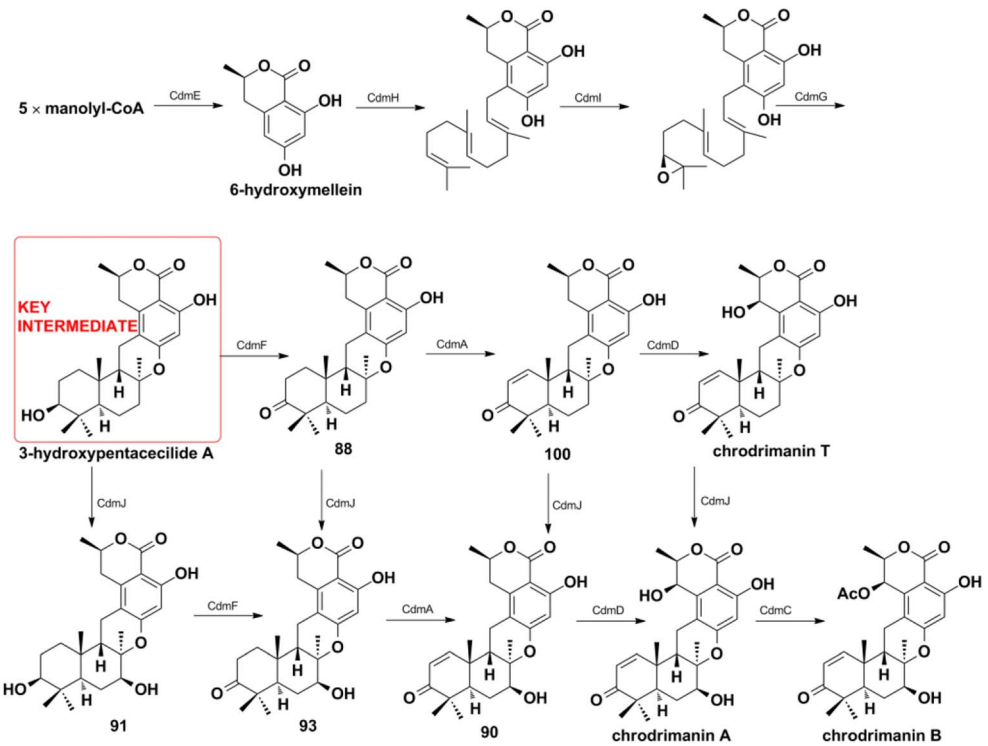

Scheme 12 Biosynthesis of chrodrimanin-type SQs.

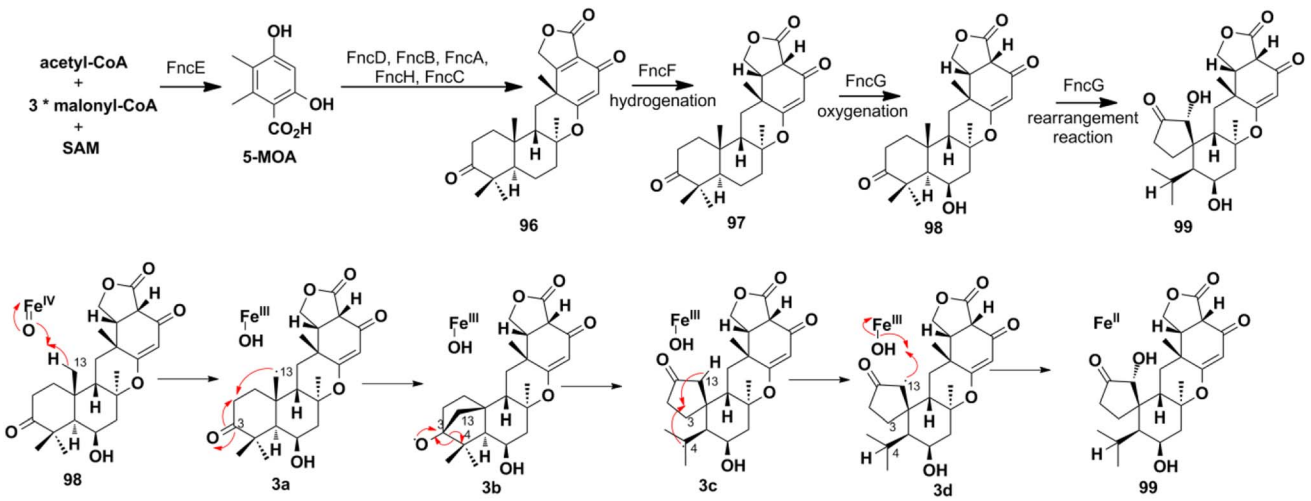

Scheme 13 Biosynthesis of funiculolide A–D (**96–99**).

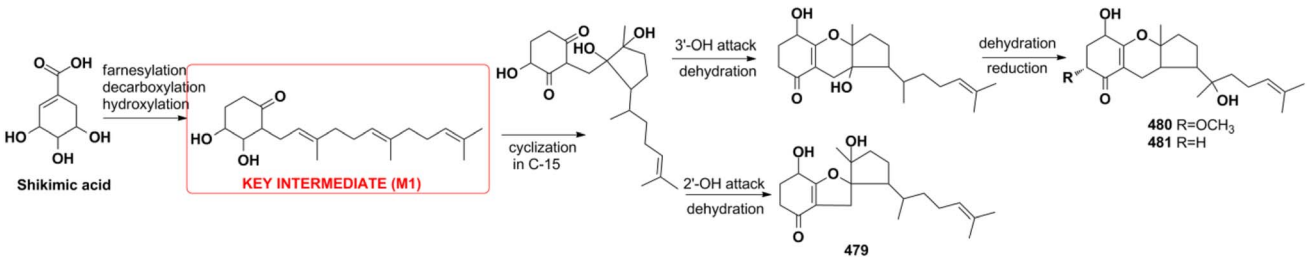

Scheme 14 Biosynthesis of tricycloalternarenes A–C (**479–481**).

NR-PKS FncE, which then undergoes FncD-catalyzed hydroxylation and lactonization, FncB-catalyzed farnesylation, FncA-catalyzed epoxidation, FncH-catalyzed cyclization, and finally alcohol dehydrogenation to construct funiculolide A (**96**).[27] Notably, FncB performs as the first prenyltransferase that dearomatizes 5-MOA with prenylation. The enoylreductase FncF is proved to be first required in the biosynthetic process of funiculolide B (**97**) by *fnc* gene cluster heterologous reconstruction. Compound **97** was oxygenated at the C-6 position to give funiculolide C (**98**) under the catalysis of FncG, a Fe(II)/α-ketoglutarate (αKG)-dependent dioxygenase. Duniculolide D (**99**) is proved to be derived from **98** *via* the ferryl-oxo-mediated bridged-ring formation reaction at C-13/C-3, β-scission at C-3/C-4, 1,4-H transfer from C-13 to C-4, and finally oxygen rebound at C-13.

4.2.4. Shikimate pathway for tricycloalternarenes A–C. Tricycloalternarenes A–C (**479–481**) are proposed to originate from the shikimate pathway by feeding experiments (Scheme 14).[151] The shikimate pathway inhibitor of 1,10-phenanthroline (PA) dose-dependently inhibits meroterpenoid production while polyketide pathway inhibitor of cerulenin has no influence. The addition of 3,4-dihydroxybenzoic acid and shikimic acid can recover the meroterpenoid production inhibited by PA. Furthermore, the presence of the key intermediate M1 was validated by the isolation of monocycloalternarenes C and D. The above experiments all proved the shikimate pathway proposed for **479–481**.

5. Conclusions and perspective

Natural SQs are hybrids of sesquiterpenoid and quinone/quinol, and they produce numerous drug candidates that are yet to be exploited. They have unique advantages in developing drug candidates for the above reasons. First is that the intrinsic structure feature makes SQs easily meet the requirement of drug-like rules. The anti-atherogenic 19-methoxy-9,15-ene-puupehenol (**109**) was reported to satisfy two more requirements for drug-like molecules with oral bioavailability according to both Veber's rule and Lipinski's rule.[78] The second is the significant bioactivity of SQs. Nearly half of all natural SQs have been proven to be active *in vitro* or *in vivo*. The third point is safety. SQs exhibit significant anti-cancer, anti-inflammatory, and anti-viral activities without affecting normal cells or tissues. The novel $sPLA_2$ inhibitor bolinaquinone acts as a potent anti-inflammatory agent on acute and chronic rat models without affecting the protective levels in other non-infected tissues and exhibits important protection against body and spleen weight loss, unlike the clinical drug dexamethasone.[207] The last feature is the multitarget features of SQs. Easily formed and highly reactive semiquinone radicals help SQs to participate in multiple pathological processes. SMTP-7 is

effective in treating thrombotic stroke in rodents and primates by modulating plasminogen conformation, which is a neuroprotective mechanism neutralizing cytokine-mediated pro-inflammation factors, reducing ROS formation and enhancing clot clearance.[145,187,188,208–212] These multitarget, multilink regulatory characteristics make SMTP-7 a possible candidate drug for thrombolytic therapy.

The only two reviews present a total of 285 marine environment SQ metabolites mostly containing the bicyclic sesquiterpenoid unit before the year 2010.[17,18] Including the 558 SQs described in this review, a total of 843 natural SQs have been discovered up to the year 2021. The increasing interest on SQs makes them increasingly important in the research area of natural products chemistry. The novel discovery strategies including multi-omics, gene cluster reconstruction, genic mutation, heterologous expression, and characteristic stereochemical, NMR, and MS features of each type of SQs provided will help accelerate SQs discovery and elucidate their structures more effectively. In the recent ten years, 60.2% new SQs were isolated from marine-derived fungi and marine organisms, implying the predominance of marine resources in new drug development. The SQs mainly distribute in relatively limited species, such as the fungi of *Stachybotrys* sp. and *Ganoderma* sp., and the sponge of *Dysidea* sp., displaying a significant chemotaxonomic role. The natural SQs are first systematically classified into seven types and sixteen subtypes in this review. Among them, the drimane-type, avarane-type, farnesane-type, and monocyclofarnesane-type occupy the largest proportion of the total SQs, accounting for 87%. All of the avarane-type SQs are produced by marine sponges, whereas most phenylspirodrimanedrimane-type and farnesane-type SQ analogs are isolated from the fungi of *Stachybotrys* and *Ganoderma*, respectively. There are many unprecedented skeletons in avarane-type SQs, and these unique metabolites indicate the amazing variety of metabolic pathways that exist in marine sponges. The phenylspirodrimanedrimane-type SQ monomers tend to dimerize in *Stachybotrys* fungi under the catalysis of specific enzymes, and these metabolic enzymes and the related functional gene clusters are worthy of further study. Many SQs possess intriguing biological and pharmacological activities, as well as fascinating structural scaffolds that are crucial for new drug development. Spiroetherone A (**262**) with unique spiro[4,5] decane skeleton exhibits combined anti-cancer effect by inhibiting angiogenesis and cancer cell proliferation.[34] Dysifragilone A (**251**) and septosone A (**264**) that featur a characteristic 6/6/6/6-fused tetracyclic ring system and pentacyclo[$6.6.2.1^{3,14}0^{1,10}0^{2,7}$] heptadecane ring system have comparable anti-inflammatory activity with that of hydrocortisone succinate and indomethacin, respectively.[36,90] SMTP-7 and dimeric FGFC1 (**553**) have been proved to be potent anti-stroke leads by dissolving thrombus *in vivo*.[182,187–189] Furthermore, the insecticidal chrodrimanins D–F (**89–91**), antimalarial phomoarcherin B (**104**), and anti-microbial SQs have significant ecological function in protecting the host from alien attack.[73,77] However, further biological studies on these compounds are severely restricted by their scarcity. The proposed biosynthetic pathways, chemical synthetic, and enzyme catalyzed biosynthetic routes outlined in this review will help solve the problem of sample scarcity. In addition, biotransformation and microbial co-cultures have provided a new approach to enrich trace constituents. More samples are needed to reveal novel bioactivity and help enhance the understanding of the pharmacokinetic, pharmacodynamics, and safety characteristics of SQs. In most studies, other important bioactivities of the SQs could not be evaluated comprehensively due to the limitation of activity testing platform and the prevalence of anti-cancer activity evaluation systems. It is also necessary to screen SQs with novel targets and strengthen the interdisciplinary cooperation between natural product chemistry and synthesis, analysis, pharmacology, and genomics.

6. Author contributions

Xin-Hui Tian: writing review and editing. Li-Li Hong & Wei-Hua Jiao: data curation. Hou-Wen Lin: project administration and supervision.

7. Conflicts of interest

There are no conflicts to declare.

8. Acknowledgements

This study was funded by National Natural Science Foundation of China (No. 82204233, 22137006, 82022068, 41906075). National Key Research and Development Program of China (No. 2022YFC2804100). Innovative Research Team of High-level Local Universities in Shanghai (No. SHSMU-ZDCX20212702).

9. References

1 R. Geris and T. J. Simpson, *Nat. Prod. Rep.*, 2009, **26**, 1063–1094.
2 M. H. Jiang, Z. E. Wu, L. Liu and S. H. Chen, *Org. Biomol. Chem.*, 2021, **19**, 1644–1704.
3 L. Minale, R. Riccio and G. Sodano, *Tetrahedron Lett.*, 1974, **38**, 3401–3404.
4 W. E. G. Muller, C. Sobel, B. Diehl-Seifert, A. Maidhof and H. C. Schroder, *Biochem. Pharmacol.*, 1987, **36**, 1489–1494.
5 P. S. Sarin, D. Sun, A. Thornton and W. E. Muller, *J. Natl. Cancer Inst.*, 1987, **78**, 663–666.
6 W. E. G. Muller, D. Sladic, R. K. Zahn, K. H. Bassler, N. Dogovic, H. Gerner, M. J. Gasic and H. C. Schroder, *Cancer Res.*, 1987, **47**, 6565–6571.
7 H. C. Schroder, R. Wenger, H. Gerner, P. Reuter, Y. Kuchino, D. Sladic and W. E. G. Muller, *Cancer Res.*, 1989, **49**, 2069–2076.
8 C. Imperatore, R. Gimmelli, M. Persico, M. Casertano, A. Guidi, F. Saccoccia, G. Ruberti, P. Luciano, A. Aiello, S. Parapini, S. Avunduk, N. Basilico, C. Fattorusso and M. Menna, *Mar. Drugs*, 2020, **18**, 112.
9 D. Sipkema, R. Osinga, W. Schatton, D. Mendola, J. Tramper and R. H. Wijffels, *Biotechnol. Bioeng.*, 2005, **90**, 201–225.

10 W. Schatton, M. Schatton and R. Pietschmann, *EU Pat.*, EP1391197B1, 2006.
11 R. T. Luibrand, T. R. Erdman, J. J. Vollmer and P. J. Scheuer, *Tetrahedron*, 1979, **35**, 609–612.
12 R. J. Capon and J. K. Macleod, *J. Org. Chem.*, 1987, **52**, 5059–5060.
13 P. A. Takizawa, J. K. Yucel, B. Veit, D. J. Faulkner, T. Deerinck, G. Soto, M. Ellisman and V. Malhotra, *Cell*, 1993, **73**, 1079–1090.
14 B. Veit, J. K. Yucel and V. Malhotra, *J. Cell Biol.*, 1993, **122**, 1197–1206.
15 S. Park, E. Yun, I. H. Hwang, S. Yoon, D. E. Kim, J. S. Kim, M. Na, G. Y. Song and S. Oh, *Mar. Drugs*, 2014, **12**, 3231–3244.
16 L. Du, Y. D. Zhou and D. G. Nagle, *J. Nat. Prod.*, 2013, **76**, 1175–1181.
17 R. J. Capon, *Stud. Nat. Prod. Chem.*, 1995, 289–326.
18 I. S. Marcos, A. Conde, R. F. Moro, P. Basabe, D. Diez and J. G. Urones, *Mini-Rev. Org. Chem.*, 2010, **7**, 230–254.
19 I. H. Hwang, J. Oh, W. Zhou, S. Park, J. H. Kim, A. G. Chittiboyina, D. Ferreira, G. Y. Song, S. Oh, M. K. Na and M. T. Hamann, *J. Nat. Prod.*, 2015, **78**, 453–461.
20 X. Zhang, T. T. Wang, Q. L. Xu, Y. Xiong, L. Zhang, H. Han, K. Xu, W. J. Guo, Q. Xu, R. X. Tan and H. M. Ge, *Angew. Chem., Int. Ed.*, 2018, **57**, 8184–8188.
21 Y. Hitora, A. Sejiyama, K. Honda, Y. Ise, F. Losung, R. E. P. Mangindaan and S. Tsukamoto, *Bioorg. Med. Chem.*, 2021, **31**, 115968.
22 J. Y. Han, J. Y. Zhang, Z. J. Song, G. L. Zhu, M. M. Liu, H. Q. Dai, T. Hsiang, X. T. Liu, L. X. Zhang, R. J. Quinn and Y. J. Feng, *Appl. Microbiol. Biotechnol.*, 2020, **104**, 3835–3846.
23 F. Zhang, M. Zhao, D. R. Braun, S. S. Ericksen, J. S. Piotrowski, J. Nelson, J. Peng, G. E. Ananiev, S. Chanana, K. Barns, J. Fossen, H. Sanchez, M. G. Chevrette, I. A. Guzei, C. G. Zhao, L. Guo, W. P. Tang, C. R. Currie, S. R. Rajski, A. Audhya, D. R. Andes and T. S. Bugni, *Science*, 2020, **370**, 974–978.
24 N. Bonneau, G. Chen, D. Lachkar, A. Boufridi, J. F. Gallard, P. Retailleau, S. Petek, C. Debitus, L. Evanno, M. A. Beniddir and E. Poupon, *Chem.–Eur. J.*, 2017, **23**, 14454–14461.
25 Y. Li, D. Liu, S. Cen, P. Proksch and W. H. Lin, *Tetrahedron*, 2014, **70**, 7010–7015.
26 Y. Yin, Q. Fu, W. H. Wu, M. H. Cai, X. S. Zhou and Y. X. Zhang, *Mar. Drugs*, 2017, **15**, 214.
27 D. X. Yan and Y. D. Matsuda, *Org. Lett.*, 2021, **23**, 3211–3215.
28 H. Qiao, S. H. Zhang, Y. Dong, Y. Yang, R. Xu, B. Chen, Y. Wang, T. J. Zhu, C. B. Cui, G. G. Zhang and C. W. Li, *Nat. Prod. Res.*, 2020, 1–8.
29 D. Arora, P. Gupta, S. Jaglan, C. Roullier, O. Grovel and S. Bertrand, *Biotechnol. Adv.*, 2020, **40**, 107521.
30 M. Menna, C. Imperatore, F. D'Aniello and A. Aiello, *Mar. Drugs*, 2013, **11**, 1602–1643.
31 P. A. García, Á. P. Hernández, A. S. Feliciano and M. Á. Castro, *Mar. Drugs*, 2018, **16**, 292.
32 M. Nazir, M. Saleem, M. I. Tousif, M. A. Anwar, F. Surup, I. Ali, D. Wang, N. Z. Mamadalieva, E. Alshammari, M. L. Ashour, A. M. Ashour, I. Ahmed, Elizbit, I. R. Green and H. Hussain, *Biomol*, 2021, **11**, 957.
33 W. H. Jiao, X. J. Huang, J. S. Yang, F. Yang, S. J. Piao, H. Gao, J. Li, W. C. Ye, X. S. Yao, W. S. Chen and H. W. Lin, *Org. Lett.*, 2012, **14**, 202–205.
34 W. H. Jiao, Q. H. Xu, J. Cui, R. Y. Shang, Y. Zhang, J. B. Sun, Q. Yang, K. C. Liu and H. W. Lin, *Org. Chem. Front.*, 2020, **7**, 368–373.
35 W. H. Jiao, T. T. Xu, H. B. Yu, G. D. Chen, X. J. Huang, F. Yang, Y. S. Li, B. N. Han, X. Y. Liu and H. W. Lin, *J. Nat. Prod.*, 2014, **77**, 346–350.
36 Y. H. Gui, W. H. Jiao, M. Zhou, Y. Zhang, D. Q. Zeng, H. R. Zhu, K. C. Liu, F. Sun, H. F. Chen and H. W. Lin, *Org. Lett.*, 2019, **21**, 767–770.
37 W. H. Jiao, B. H. Cheng, G. D. Chen, G. H. Shi, J. Li, T. Y. Hu and H. W. Lin, *Org. Lett.*, 2018, **20**, 3092–3095.
38 K. Kawashima, K. Nakanishi and H. Nishikawa, *Chem. Pharm. Bull.*, 1964, **12**, 796–803.
39 S. M. Fang, C. B. Cui, C. W. Li, C. J. Wu, Z. J. Zhang, L. Li, X. J. Huang and W. C. Ye, *Mar. Drugs*, 2012, **10**, 1266–1287.
40 X. P. Lin, Q. Y. Wu, Y. Y. Yu, Z. Liang, Y. H. Liu, L. L. Zhou, L. Tang and X. F. Zhou, *Sci. Rep.*, 2017, **7**, 10757.
41 X. P. Lin, X. F. Zhou, F. Z. Wang, K. S. Liu, B. Yang, X. W. Yang, Y. Peng, J. Liu, Z. Ren and Y. H. Liu, *Mar. Drugs*, 2012, **10**, 106–115.
42 Y. Fu, P. Wu, J. H. Xue and X. Y. Wei, *J. Nat. Prod.*, 2014, **77**, 1791–1799.
43 Y. Fu, P. Wu, J. H. Xue, H. X. Li and X. Y. Wei, *Mar. Drugs*, 2015, **13**, 3360–3367.
44 L. Zhang, Y. Shen, F. Wang, Y. Leng and J. K. Liu, *Phytochemistry*, 2010, **71**, 100–103.
45 C. J. Zheng, C. L. Shao, M. Chen, Z. G. Niu, D. L. Zhao and C. Y. Wang, *Chem. Biodiversity*, 2015, **12**, 1407–1414.
46 C. Li, D. H. Li, S. X. Cai, F. P. Wang, X. Xiao and Q. G. Gu, *Acta Pharmacol. Sin.*, 2010, **45**, 1275–1278.
47 L. E. Schmidt, S. T. Deyrup, J. Baltrusaitis, D. C. Swenson, D. T. Wicklow and J. B. Gloer, *J. Nat. Prod.*, 2010, **73**, 404–408.
48 A. Hirose, H. Maeda, A. Tonouchi, T. Nehira and M. Hashimoto, *Tetrahedron*, 2014, **70**, 1458–1463.
49 I. E. Mohamed, S. Kehraus, A. Krick, G. M. Konig, G. Kelter, A. Maier, H. H. Fiebig, M. Kalesse, N. P. Malek and H. Gross, *J. Nat. Prod.*, 2010, **73**, 2053–2056.
50 C. J. Chen, Y. Q. Zhou, X. X. Liu, W. J. Zhang, S. S. Hu, L. P. Lin, G. M. Huo, R. H. Jiao, R. X. Tan and H. M. Ge, *Tetrahedron Lett.*, 2015, **56**, 6183–6189.
51 A. L. Lane, L. Mular, E. J. Drenkard, T. L. Shearer, S. Engel, S. Fredericq, C. R. Fairchild, J. Prudhomme, K. L. Roch, M. E. Hay, W. Aalbersberg and J. Kubanek, *Tetrahedron*, 2010, **66**, 455–461.
52 K. Chakraborty, T. Antony and M. Joy, *Algal Res.*, 2019, **40**, 101472.
53 F. Ishibashi, S. Sato, K. Sakai, S. Hirao and K. Kuwano, *Biosci., Biotechnol., Biochem.*, 2013, **77**, 1120–1122.
54 M. Kumagai, K. Nishikawa, H. Matsuura, T. Umezawa, F. Matsuda and T. Okino, *Molecules*, 2018, **23**, 1214.

55 X. Zhang, H. Y. Xu, A. M. Huang, L. Wang, Q. Wang, P. Y. Cao and P. M. Yang, *Chem. Pharm. Bull.*, 2016, **64**, 1036–1042.
56 L. K. Shubina, A. I. Kalinovsky, T. N. Makarieva, S. N. Fedorov, S. A. Dyshlovoy, P. S. Dmitrenok, I. I. Kapustina, E. Mollo, N. K. Utkina, V. B. Krasokhin, V. A. Denisenko and V. A. Stonik, *Nat. Prod. Commun.*, 2012, **7**, 487–490.
57 H. Liu, X. M. Li, Y. Liu, P. Zhang, J. N. Wang and B. G. Wang, *J. Nat. Prod.*, 2016, **79**, 806–811.
58 A. R. Wang, Y. B. Xu, Y. X. Gao, Q. Huang, X. Luo, H. M. An and J. Y. Dong, *Phytochem. Rev.*, 2015, **14**, 623–655.
59 B. Wu, V. Oesker, J. Wiese, S. Malien, R. Schmaljohann and J. F. Imhoff, *Mar. Drugs*, 2014, **12**, 1924–1938.
60 J. L. Zhao, J. M. Feng, Z. Tan, J. M. Liu, J. Y. Zhao, R. D. Chen, K. B. Xie, D. W. Zhang, Y. Li, L. Y. Yu, X. G. Chen and J. G. Dai, *J. Nat. Prod.*, 2017, **80**, 1819–1826.
61 J. L. Zhao, J. M. Liu, Y. Shen, Z. Tan, M. Zhang, R. D. Chen, J. Y. Zhao, D. W. Zhang, L. Y. Yu and J. G. Dai, *Phytochem. Lett.*, 2017, **20**, 289–294.
62 D. Liu, Y. Li, X. D. Li, Z. B. Cheng, J. Huang, P. Proksch and W. H. Lin, *Tetrahedron Lett.*, 2017, **58**, 1826–1829.
63 Y. Li, C. M. Wu, D. Liu, P. Proksch, P. Guo and W. H. Lin, *J. Nat. Prod.*, 2014, **77**, 138–147.
64 X. H. Ma, L. T. Li, T. J. Zhu, M. Y. Ba, G. Q. Li, Q. Q. Gu, Y. Guo and D. H. Li, *J. Nat. Prod.*, 2013, **76**, 2298–2306.
65 P. P. Zhang, Y. F. Li, C. X. Jia, J. J. Lang, S. I. Niaz, J. Li, J. Yuan, J. C. Yu, S. H. Chen and L. Liu, *RSC Adv.*, 2017, **7**, 49910.
66 W. X. Chunyu, Z. G. Ding, M. G. Li, J. Y. Zhao, S. J. Gu, Y. Gao, F. Wang, J. H. Ding and M. L. Wen, *Helv. Chim. Acta*, 2016, **99**, 583–587.
67 H. Zhang, M. H. Yang, F. F. Zhuo, N. Gao, X. B. Cheng, X. B. Wang, Y. H. Pei and L. Y. Kong, *RSC Adv.*, 2019, **9**, 3520.
68 M. X. Hua, W. M. Zheng, K. H. Sun, X. F. Gu, X. M. Zeng, H. T. Zhang, T. H. Zhong, Z. Z. Shao and Y. H. Zhang, *Nat. Prod. Res.*, 2019, **33**, 386–392.
69 J. W. Kim, S. K. Ko, H. M. Kim, G. H. Kim, S. Son, G. S. Kim, G. J. Hwang, E. S. Jeon, K. S. Shin, I. J. Ryoo, Y. S. Hong, H. Oh, K. H. Lee, N. K. Soung, D. Hashizume, T. Nogawa, S. Takahashi, B. Y. Kim, H. Osada, J. H. Jang and J. S. Ahn, *J. Nat. Prod.*, 2016, **79**, 2703–2708.
70 Y. C. Xu, C. Wang, H. S. Liu, G. L. Zhu, P. Fu, L. P. Wang and W. M. Zhu, *Mar. Drugs*, 2018, **16**, 363.
71 D. Zhou, L. J. Li, H. Qi, J. J. Pan, H. Zhang, J. D. Wang and W. S. Xiang, *J. Antibiot.*, 2015, **68**, 339–341.
72 H. Hayashi, Y. Oka, K. Kai and K. Akiyama, *Biosci., Biotechnol., Biochem.*, 2012, **76**, 745–748.
73 H. Hayashi, Y. Oka, K. Kai and K. Akiyama, *Biosci., Biotechnol., Biochem.*, 2012, **76**, 1765–1768.
74 T. El-Elimat, M. Figueroa, H. A. Raja, S. Alnabulsi and N. H. Oberlies, *Tetrahedron Lett.*, 2021, **72**, 153067.
75 Y. M. Fu, C. H. Li, J. Zhu, L. T. Zhang, Y. Wang, Q. L. Chen, L. Xu, S. Y. Zhang, Y. Fang and T. Liu, *Biochem. Syst. Ecol.*, 2020, **93**, 104186.
76 H. Yamazaki, W. Nakayama, O. Takahashi, R. Kirikoshi, Y. Izumikawa, K. Iwasaki, K. Toraiwa, K. Ukai, H. Rotinsulu, D. S. Wewengkang, D. A. Sumilat, R. E. P. Mangindaan and M. Namikoshi, *Bioorg. Med. Chem. Lett.*, 2015, **25**, 3087–3090.
77 C. Hemtasin, S. Kanokmedhakul, K. Kanokmedhakul, C. Hahnvajanawong, K. Soytong, S. Prabpai and P. Kongsaeree, *J. Nat. Prod.*, 2011, **74**, 609–613.
78 H. A. Wahab, N. B. Pham, T. S. T. Muhammad, J. N. A. Hooper and R. J. Quinn, *Mar. Drugs*, 2017, **15**, 1–10.
79 J. Li, B. B. Gu, F. Sun, J. R. Xu, W. H. Jiao, H. B. Yu, B. N. Han, F. Yang, X. C. Zhang and H. W. Lin, *J. Nat. Prod.*, 2017, **80**, 1436–1445.
80 K. Hagiwara, J. E. G. Hernandez, M. K. Harper, A. Carroll, C. A. Motti, J. Awaya, H. Y. Nguyen and A. D. Wright, *J. Nat. Prod.*, 2015, **78**, 325–329.
81 Q. Göthel and M. Köck, *Beilstein J. Org. Chem.*, 2014, **10**, 613–621.
82 V. R. D. L. Parra, V. Mierau, T. Anke and O. Sterner, *Tetrahedron*, 2006, **62**, 1828–1832.
83 L. Flores-Bocanegra, M. Augustinovic, H. A. Raja, S. J. Kurina, A. C. Maldonado, J. E. Burdette, J. O. Falkinham, C. J. Pearce and N. H. Oberlies, *Tetrahedron Lett.*, 2021, **68**, 152896.
84 J. Li, F. Yang, Z. Wang, W. Wu, L. Liu, S. P. Wang, B. X. Zhao, W. H. Jiao, S. H. Xu and H. W. Lin, *Org. Biomol. Chem.*, 2018, **16**, 6773–6782.
85 P. L. Winder, H. L. Baker, P. Linley, E. A. Guzmán, S. A. Pomponi, M. C. Diaz, J. K. Reed and A. E. Wright, *Bioorg. Med. Chem.*, 2011, **19**, 6599–6603.
86 J. Li, W. Wu, F. Yang, L. Liu, S. P. Wang, W. H. Jiao, S. H. Xu and H. W. Lin, *Chem. Biodiversity*, 2018, **15**, e1800078.
87 W. H. Jiao, T. T. Xu, B. B. Gu, G. H. Shi, Y. Zhu, F. Yang, B. N. Han, S. P. Wang, Y. S. Li, W. Zhang, J. Li and H. W. Lin, *RSC Adv.*, 2015, **5**, 87730–87738.
88 Y. H. Gui, L. Liu, W. Wu, Y. Zhang, Z. L. Jia, Y. P. Shi, H. T. Kong, K. C. Liu, W. H. Jiao and H. W. Lin, *Bioorg. Chem.*, 2020, **94**, 103435.
89 L. Liu, W. Wu, J. Li, W. H. Jiao, L. Y. Liu, J. Tang, L. Liu, F. Sun, B. N. Han and H. W. Lin, *Biomed. Pharmacother.*, 2018, **100**, 417–425.
90 W. H. Jiao, T. T. Xu, F. Zhao, H. Gao, G. H. Shi, J. Wang, L. L. Hong, H. B. Yu, Y. S. Li, F. Yang and H. W. Lin, *Eur. J. Org. Chem.*, 2015, **2015**, 960–966.
91 J. Tang, W. Wu, F. Yang, L. Y. Liu, Z. Yang, L. Liu, W. Z. Tang, F. Sun and H. W. Lin, *Cancer Med.*, 2018, **7**, 3965–3976.
92 W. H. Jiao, G. H. Shi, T. T. Xu, G. D. Chen, B. B. Gu, Z. Wang, S. Peng, S. P. Wang, J. Li, B. N. Han, W. Zhang and H. W. Lin, *J. Nat. Prod.*, 2016, **79**, 406–411.
93 W. H. Jiao, T. T. Xu, H. B. Yu, F. R. Mu, J. Li, Y. S. Li, F. Yang, B. N. Han and H. W. Lin, *RSC Adv.*, 2014, **4**, 9236.
94 W. H. Jiao, J. Li, D. Wang, M. M. Zhang, L. Y. Liu, F. Sun, J. Y. Li, R. J. Capon and H. W. Lin, *J. Nat. Prod.*, 2019, **82**, 2586–2593.

95 W. H. Jiao, B. H. Cheng, G. H. Shi, G. D. Chen, B. B. Gu, Y. J. Zhou, L. L. Hong, F. Yang, Z. Q. Liu, S. Q. Qiu, Z. G. Liu, P. C. Yang and H. W. Lin, *Sci. Rep.*, 2017, **7**, 8947.
96 J. Wang, F. R. Mu, W. H. Jiao, J. Huang, L. L. Hong, F. Yang, Y. Xu, S. P. Wang, F. Sun and H. W. Lin, *J. Nat. Prod.*, 2017, **80**, 2509–2514.
97 W. H. Jiao, J. Li, M. M. Zhang, J. Cui, Y. H. Gui, Y. Zhang, J. Y. Li, K. C. Liu and H. W. Lin, *Org. Lett.*, 2019, **21**, 6190–6193.
98 H. B. Yu, Z. F. Yin, B. B. Gu, J. P. Zhang, S. P. Wang, F. Yang and H. W. Lin, *Nat. Prod. Res.*, 2021, **35**, 1620–1626.
99 H. X. Li, Q. Zhang, X. Jin, X. W. Zou, Y. X. Wang, D. X. Hao, F. H. Fu, W. H. Jiao, C. X. Zhang, H. W. Lin, K. Matsuzaki and F. Zhao, *Mol. Med. Rep.*, 2018, **17**, 674–682.
100 R. A. Hill and A. Sutherland, *Nat. Prod. Rep.*, 2018, **35**, 702–706.
101 R. A. Hill and A. Sutherland, *Nat. Prod. Rep.*, 2019, **36**, 556–560.
102 R. A. Hill and A. Sutherland, *Nat. Prod. Rep.*, 2019, **36**, 1378–1382.
103 R. A. Hill and A. Sutherland, *Nat. Prod. Rep.*, 2012, **29**, 435–439.
104 R. A. Hill and A. Sutherland, *Nat. Prod. Rep.*, 2014, **31**, 706–710.
105 G. Daletos, N. J. D. Voogd, W. E. G. Müller, V. Wray, W. H. Lin, D. Feger, M. Kubbutat, A. H. Aly and P. Proksch, *J. Nat. Prod.*, 2014, **77**, 218–226.
106 S. P. B. Ovenden, J. L. Nielson, C. H. Liptrot, R. H. Willis, D. M. Tapiolas, A. D. Wright and C. A. Motti, *J. Nat. Prod.*, 2011, **74**, 65–68.
107 W. Balansa, U. Mettal, Z. G. Wuisan, A. Plubrukarn, F. G. Ijong, Y. Liu and T. F. Schäberle, *Mar. Drugs*, 2019, **17**, 158.
108 A. N. E. S. Hamed, W. Wätjen, R. Schmitz, Y. Chovolou, R. A. Edrada-Ebel, D. T. A. Youssef, M. S. Kamel and P. Proksch, *Nat. Prod. Commun.*, 2013, **8**, 289–292.
109 C. K. Kim, J. K. Woo, S. H. Kim, E. Cho, Y. J. Lee, H. S. Lee, C. J. Sim, D. C. Oh, K. B. Oh and J. Shin, *J. Nat. Prod.*, 2015, **78**, 2814–2821.
110 X. C. Luo, P. L. Li, K. Y. Wang, N. J. D. Voogd, X. L. Tang and G. Q. Li, *Nat. Prod. Res.*, 2021, **35**, 2866–2871.
111 D. B. Abdjul, H. Yamazaki, O. Takahashi, R. Kirikoshi, K. Ukai and M. Namikoshi, *J. Nat. Prod.*, 2016, **79**, 1842–1847.
112 N. K. Utkina, V. A. Denisenko and V. B. Krasokhin, *J. Nat. Prod.*, 2010, **73**, 788–791.
113 Y. Takahashi, M. Ushio, T. Kubota, S. Yamamoto, J. Fromont and J. Kobayashi, *J. Nat. Prod.*, 2010, **73**, 467–471.
114 H. M. Nguyen, T. Ito, N. N. Win, T. Kodama, V. Q. Hung, H. T. Nguyen and H. Morita, *Phytochem. Lett.*, 2016, **17**, 288–292.
115 H. M. Nguyen, T. Ito, S. Kurimoto, M. Ogawa, N. N. Win, V. Q. Hung, H. T. Nguyen, T. Kubota, J. Kobayashi and H. Morita, *Bioorg. Med. Chem. Lett.*, 2017, **27**, 3043–3047.
116 T. Ito, H. M. Nguyen, N. N. Win, H. Q. Vo, H. T. Nguyen and H. Morita, *J. Nat. Med.*, 2018, **72**, 298–303.
117 P. V. Kiem, L. T. Huyen, D. T. Hang, N. X. Nhiem, B. H. Tai, H. L. T. Anh, P. V. Cuong, T. H. Quang, C. V. Minh, N. V. Dau, Y. A. Kim, L. Subedi, S. Y. Kim and S. H. Kim, *Bioorg. Med. Chem. Lett.*, 2017, **27**, 1525–1529.
118 H. Mitome, T. Nagasawa, H. Miyaoka, Y. Yamada and R. W. M. V. Soest, *J. Nat. Prod.*, 2001, **64**, 1506–1508.
119 H. Mitome, T. Nagasawa, H. Miyaoka, Y. Yamada and R. W. M. V. Soest, *Tetrahedron*, 2002, **58**, 1693–1696.
120 L. T. Huyen, D. T. Hang, N. X. Nhiem, B. H. Tai, H. L. T. Anh, T. H. Quang, P. H. Yen, C. V. Minh, N. V. Dau and P. V. Kiem, *Nat. Prod. Commun.*, 2017, **12**, 477–478.
121 J. Baars, I. Grimm, D. Blunk, J. M. Neudörfl and H. G. Schmalz, *Angew. Chem., Int. Ed.*, 2021, **60**, 14915–14920.
122 C. K. Chong, Q. L. Zhang, J. Ke, H. M. Zhang, X. D. Yang, B. J. Wang, W. Ding and Z. Y. Lu, *Angew. Chem., Int. Ed.*, 2021, **60**, 13807–13813.
123 H. Prawat, C. Mahidol, W. Kaweetripob, S. Wittayalai and S. Ruchirawat, *Tetrahedron*, 2012, **68**, 6881–6886.
124 W. W. Cao, Q. Luo, Y. X. Cheng and S. M. Wang, *Fitoterapia*, 2016, **110**, 110–115.
125 F. J. Zhou, Y. Nian, Y. M. Yan, Y. Gong, Q. Luo, Y. Zhang, B. Hou, Z. L. Zuo, S. M. Wang, H. H. Jiang, J. Yang and Y. X. Cheng, *Org. Lett.*, 2015, **17**, 3082–3085.
126 F. Y. Qin, Y. M. Yan, Z. C. Tu and Y. X. Cheng, *J. Asian Nat. Prod. Res.*, 2019, **21**, 542–550.
127 Y. P. Li, X. T. Jiang, F. Y. Qin, H. X. Zhang and Y. X. Cheng, *Bioorg. Chem.*, 2021, **109**, 104706.
128 L. Z. Cheng, F. Y. Qin, X. C. Ma, S. M. Wang, Y. M. Yan and Y. X. Cheng, *Molecules*, 2018, **23**, 1797.
129 M. Dou, R. T. Li and Y. X. Cheng, *Chin. Herb. Med.*, 2016, **8**, 85–88.
130 X. L. Wang, Z. H. Wu, L. Di, F. J. Zhou, Y. M. Yan and Y. X. Cheng, *Phytochemistry*, 2019, **162**, 199–206.
131 X. L. Wang, F. J. Zhou, M. Dou, Y. M. Yan, S. M. Wang, L. Di and Y. X. Cheng, *Bioorg. Med. Chem. Lett.*, 2016, **26**, 5507–5512.
132 Q. Luo, Z. L. Yang and Y. X. Cheng, *Tetrahedron*, 2019, **75**, 2910–2915.
133 J. J. Zhang, F. Y. Qin, X. H. Meng, Y. M. Yan and Y. X. Cheng, *Bioorg. Chem.*, 2020, **100**, 103930.
134 Q. Luo, X. L. Wang, L. Di, Y. M. Yan, Q. Lu, X. H. Yang, D. B. Hu and Y. X. Cheng, *Tetrahedron*, 2015, **71**, 840–845.
135 D. Cai, J. J. Zhang, Z. H. Wu, F. Y. Qin, Y. M. Yan, M. Zhang and Y. X. Cheng, *Bioorg. Chem.*, 2021, **110**, 104774.
136 X. H. Meng, F. Y. Qin, X. T. Jiang, Y. Li and Y. X. Cheng, *Bioorg. Chem.*, 2021, **112**, 104950.
137 J. C. Guo, F. D. Kong, Q. Y. Ma, Q. Y. Xie, R. S. Zhang, H. F. Dai, Y. G. Wu and Y. X. Zhao, *Front. Chem.*, 2020, **8**, 279.
138 X. R. Peng, J. Q. Liu, C. F. Wang, Z. H. Han, Y. Shu, X. Y. Li, L. Zhou and M. H. Qiu, *Food Chem.*, 2015, **171**, 251–257.
139 X. R. Peng, X. Wang, L. Chen, H. Yang, L. Li, S. Y. Lu, L. Zhou and M. H. Qiu, *Fitoterapia*, 2018, **127**, 286–292.

140 M. Adams, M. Christen, I. Plitzko, S. Zimmermann, R. Brun, M. Kaiser and M. Hamburger, *J. Nat. Prod.*, 2010, **73**, 897–900.
141 J. C. Guo, Q. Y. Ma, F. D. Kong, Q. Y. Xie, L. M. Zhou, Q. Ding, Y. G. Wu and Y. X. Zhao, *Chin. J. Org. Chem.*, 2019, **39**, 3264–3268.
142 X. Q. Chen, L. X. Chen, S. P. Li and J. Zhao, *Phytochem. Lett.*, 2017, **22**, 214–218.
143 X. H. Ma, H. T. Wang, F. Li, T. J. Zhu, Q. Q. Gu and D. H. Li, *Tetrahedron*, 2015, **56**, 7053–7055.
144 R. H. Guo, Y. T. Zhang, D. Duan, Q. Fu, X. Y. Zhang, X. W. Yu, S. J. Wang, B. Bao and W. H. Wu, *Chin. J. Chem.*, 2016, **34**, 1194–1198.
145 H. Koide, K. Hasegawa, N. Nishimura, R. Narasaki and K. Hasumi, *J. Antibiot.*, 2012, **65**, 361–367.
146 K. Hasegawa, H. Koide, W. M. Hu, N. Nishimura, R. Narasaki, Y. Kitano and K. Hasumi, *J. Antibiot.*, 2010, **63**, 589–593.
147 H. Koide, R. Narasaki, K. Hasegawa, N. Nishimura and K. Hasumi, *J. Antibiot.*, 2012, **65**, 91–93.
148 Y. Nishimura, E. Suzuki, K. Hasegawa, N. Nishimura, Y. Kitano and K. Hasumi, *J. Antibiot.*, 2012, **65**, 483–485.
149 M. Akiba, K. Kinoshita, Y. Kino, J. Sato and K. Koyama, *Bioorg. Med. Chem. Lett.*, 2020, **30**, 126808.
150 Y. Masuda, K. Fujihara, S. Hayashi, H. Sasaki, Y. Kino, H. Kamauchi, M. Noji, J. Satoh, T. Takanami, K. Kinoshita and K. Koyama, *J. Nat. Prod.*, 2021, **84**, 1748–1754.
151 G. J. Zhang, G. W. Wu, T. J. Zhu, T. Kurtán, A. Mándi, J. Y. Jiao, J. Li, X. Qi, Q. Q. Gu and D. H. Li, *J. Nat. Prod.*, 2013, **76**, 1946–1957.
152 X. Shi, W. Wei, W. J. Zhang, C. P. Hua, C. J. Chen, H. M. Ge, R. X. Tan and R. H. Jiao, *J. Asian Nat. Prod. Res.*, 2015, **17**, 143–148.
153 Q. Shi, T. T. Li, Y. M. Wu, X. Y. Sun, C. Lei, J. Y. Li and A. J. Hou, *Phytochemistry*, 2020, **180**, 112524.
154 Y. Long, T. Tang, L. Y. Wang, B. He and K. Gao, *J. Nat. Prod.*, 2019, **82**, 2229–2237.
155 Y. Long, T. Tang, L. Y. Wang, B. He and K. Gao, *J. Nat. Prod.*, 2019, **82**, 3205.
156 D. S. Manamgoda, L. Cai, A. H. Bahkali, E. Chukeatirote and K. D. Hyde, *Fungal Diversity*, 2011, **51**, 3–42.
157 M. Wang, Z. H. Sun, Y. C. Chen, H. X. Liu, H. H. Li, G. H. Tan, S. N. Li, X. L. Guo and W. M. Zhang, *Fitoterapia*, 2016, **110**, 77–82.
158 Q. Y. Qi, L. Huang, L. W. He, J. J. Han, Q. Chen, L. Cai and H. W. Liu, *Chem. Biodiversity*, 2014, **11**, 1892–1899.
159 X. Cao, Y. T. Shi, X. D. Wu, K. W. Wang, S. H. Huang, H. X. Sun, J. S. Dickschat and B. Wu, *Org. Lett.*, 2019, **21**, 6539–6542.
160 X. Cao, Y. T. Shi, S. H. Wu, X. D. Wu, K. W. Wang, H. X. Sun, S. He, J. S. Dickschat and B. Wu, *Tetrahedron*, 2020, **76**, 131349.
161 Y. Hitora, K. Takada, Y. Ise, S. P. Woo, S. Inoue, N. Mori, H. Takikawa, S. Nakamukai, S. Okada and S. Matsunaga, *Bioorg. Med. Chem.*, 2020, **28**, 115233.
162 S. P. B. Ovenden, J. L. Nielson, C. H. Liptrot, R. H. Willis, D. M. Tapiolas, A. D. Wright and C. A. Motti, *J. Nat. Prod.*, 2011, **74**, 1335–1338.
163 Y. X. Song, H. B. Huang, Y. C. Chen, J. Ding, Y. Zhang, A. J. Sun, W. M. Zhang and J. H. Ju, *J. Nat. Prod.*, 2013, **76**, 2263–2268.
164 F. L. Li, Y. Tang, W. G. Sun, J. K. Guan, Y. Y. Lu, S. T. Zhang, S. Lin, J. P. Wang, Z. X. Hu and Y. H. Zhang, *Bioorg. Chem.*, 2019, **92**, 103279.
165 L. Wang, J. Y. Jiao, D. Liu, X. M. Zhang, J. Li, Q. Che, T. J. Zhu, G. J. Zhang and D. H. Li, *Chem. Biodiversity*, 2020, **17**, e2000226.
166 U. Sommart, V. Rukachaisirikul, K. Trisuwan, K. Tadpetch, S. Phongpaichit, S. Preedanon and J. Sakayaroj, *Phytochem. Lett.*, 2012, **5**, 139–143.
167 M. Carbone, L. Nunez-Pons, M. Paone, F. Castelluccio, C. Avila and M. Gavagnin, *Tetrahedron*, 2012, **68**, 3541–3544.
168 M. Carbone, L. Nunez-Pons, M. Paone, F. Castelluccio, C. Avila and M. Gavagnin, *Tetrahedron*, 2012, **68**, 8515.
169 M. Dou, L. Di, L. L. Zhou, Y. M. Yan, X. L. Wang, F. J. Zhou, Z. L. Yang, R. T. Li, F. F. Hou and Y. X. Cheng, *Org. Lett.*, 2014, **16**, 6064–6067.
170 G. H. Huang, C. Lei, K. X. Zhu, J. Y. Li, J. Li and A. J. Hou, *Chin. J. Nat. Med.*, 2019, **17**, 0963–0969.
171 Z. J. Zhan, Y. M. Ying, L. F. Ma and W. G. Shan, *Nat. Prod. Rep.*, 2011, **28**, 594–629.
172 L. F. Ma, Y. L. Chen, W. G. Shan and Z. J. Zhan, *Nat. Prod. Rep.*, 2020, **37**, 999–1030.
173 Y. H. Ma, X. X. Dou and X. H. Tian, *Phytochem. Rev.*, 2020, **19**, 983–1043.
174 N. K. Utkina, V. A. Denisenko and V. B. Krasokhin, *Tetrahedron Lett.*, 2011, **52**, 3765–3768.
175 J. M. Liu, X. N. Jia, J. L. Zhao, J. M. Feng, M. H. Chen, R. D. Chen, K. B. Xie, D. W. Chen, Y. Li, D. Zhang, Y. Peng, S. Y. Si and J. G. Dai, *Org. Chem. Front.*, 2020, **7**, 531–542.
176 J. M. Feng, M. Zhang, X. N. Jia, J. L. Zhao, R. D. Chen, K. B. Xie, D. W. Chen, Y. Li, J. M. Liu and J. G. Dai, *Fitoterapia*, 2019, **136**, 104158.
177 J. L. Zhao, J. M. Feng, Z. Tan, J. M. Liu, M. Zhang, R. D. Chen, K. B. Xie, D. W. Chen, Y. Li, X. G. Chen and J. G. Dai, *Bioorg. Med. Chem. Lett.*, 2018, **28**, 355–359.
178 M. Zhang, J. M. Feng, X. N. Jia, J. L. Zhao, J. M. Liu, R. D. Chen, K. B. Xie, D. W. Chen, Y. Li, D. Zhang and J. G. Dai, *Chin. Chem. Lett.*, 2019, **30**, 435–438.
179 Z. G. Ding, J. H. Ding, J. Y. Zhao, W. X. Chunyu, M. G. Li, S. J. Gu, F. Wang and M. L. Wen, *Fitoterapia*, 2018, **125**, 94–97.
180 Z. G. Ding, J. Y. Zhao, J. H. Ding, W. X. Chunyu, M. G. Li, S. J. Gu, F. Wang and M. L. Wen, *Nat. Prod. Res.*, 2018, **32**, 2370–2374.
181 D. Liu, Y. Li, X. C. Guo, W. Ji and W. H. Lin, *Chem. Biodiversity*, 2020, **17**, e2000170.
182 G. Wang, W. H. Wu, Q. G. Zhu, S. Q. Fu, X. Y. Wang, S. T. Hong, R. H. Guo and B. Bao, *Chin. J. Chem.*, 2015, **33**, 1089–1095.

183 M. Amigó, M. Payá, A. Braza-Boïls, S. D. Rosa and M. C. Terencio, *Life Sci.*, 2008, **82**, 256–264.
184 M. L. Ferrandiz, M. J. Sanz, G. Bustos, M. Payfi, M. J. Alcaraz and S. D. Rosa, *Eur. J. Pharmacol.*, 1994, **253**, 75–82.
185 W. E. G. Muller, A. Maidhof, R. K. Zahn, H. C. Schroder, M. J. Gasic, D. Heidemann, A. Bernd, B. Kurelec, E. Eich and G. Seibert, *Cancer Res.*, 1985, **45**, 4822–4826.
186 J. M. Miguel del Corral, M. Gordaliza, M. A. Castro, M. M. Mahiques, P. Chamorro, A. Molinari, M. D. García-Grávalos, H. B. Broughton and A. S. Feliciano, *J. Med. Chem.*, 2001, **44**, 1257–1267.
187 T. Hashimoto, K. Shibata, K. Nobe, K. Hasumi and K. Honda, *J. Pharmacol. Sci.*, 2010, **114**, 41–49.
188 T. Miyazaki, Y. Kimura, H. Ohata, T. Hashimoto, K. Shibata, K. Hasumi and K. Honda, *Stroke*, 2011, **42**, 1097–1104.
189 T. Yan, W. H. Wu, T. W. Su, J. J. Chen, Q. G. Zhu, C. Y. Zhang, X. Y. Wang and B. Bao, *Arch. Pharmacal Res.*, 2015, **38**, 1530–1540.
190 T. T. Ling, A. X. Xiang and E. A. Theodorakis, *Angew. Chem., Int. Ed.*, 1999, **20**, 3089–3091.
191 T. T. Ling, E. Poupon, E. J. Rueden, S. H. Kim and E. A. Theodorakis, *J. Am. Chem. Soc.*, 2002, **124**, 12261–12267.
192 E. P. Locke and S. M. Hecht, *Chem. Commun.*, 1996, **24**, 2717–2718.
193 A. S. Sarma and P. Chattopadhyay, *J. Org. Chem.*, 1982, **47**, 1727–1731.
194 J. Sakurai, T. Oguchi, K. Watanabe, H. Abe, S. I. Kanno, M. Ishikawa and T. Katoh, *Chem.–Eur. J.*, 2008, **14**, 829–837.
195 J. H. George, *Acc. Chem. Res.*, 2021, **54**, 1843–1855.
196 T. X. Bai, Z. Y. Quan, R. Zhai, T. Awakawa, Y. Matsuda and I. Abe, *Org. Lett.*, 2018, **20**, 7504–7508.
197 S. M. Shen, G. Appendino and Y. W. Guo, *Nat. Prod. Rep.*, 2022, **39**, 1803–1832.
198 C. K. Chong and Z. Y. Lu, *Synlett*, 2021, **32**, 1777–1783.
199 X. Yin, M. Mato and A. M. Echavarren, *Angew. Chem., Int. Ed.*, 2017, **56**, 14591–14595.
200 X. Yin, M. Mato and A. M. Echavarren, *Angew. Chem.*, 2017, **129**, 14783–14787.
201 M. A. Haque and C. K. Jana, *Chem.–Eur. J.*, 2017, **23**, 13300–13304.
202 M. A. Haque and C. K. Jana, *Chem.–Eur. J.*, 2019, **25**, 12849.
203 M. A. Haque, B. L. Sailo, G. Padmavathi, A. B. Kunnumakkara and C. K. Jana, *Eur. J. Med. Chem.*, 2018, **160**, 256–265.
204 S. De, E. Mahal, M. A. Haque, C. K. Jana and D. Koley, *J. Org. Chem.*, 2021, **86**, 1133–1140.
205 Y. Fukui, K. Narita and T. Katoh, *Chem.–Eur. J.*, 2014, **20**, 2436–2439.
206 B. Schmalzbauer, J. Herrmann, R. Muller and D. Menche, *Org. Lett.*, 2013, **15**, 964–967.
207 R. Lucas, C. Giannini, M. V. D'Auria and M. Paya, *J. Pharmacol. Exp. Ther.*, 2003, **304**, 1172–1180.
208 K. Shibata, T. Hashimoto, K. Nobe, K. Hasumi and K. Honda, *Naunyn-Schmiedeberg's Arch. Pharmacol.*, 2011, **384**, 103–108.
209 Y. Akamatsu, A. Saito, M. Fujimura, H. Shimizu, M. Mekawy, K. Hasumi and T. Tominaga, *Neurosci. Lett.*, 2011, **503**, 110–114.
210 K. Shibata, T. Hashimoto, K. Nobe, K. Hasumi and K. Honda, *Naunyn-Schmiedeberg's Arch. Pharmacol.*, 2010, **382**, 245–253.
211 W. M. Hu, R. Narasaki, N. Nishimura and K. Hasumi, *Thromb. J.*, 2012, **10**, 1–9.
212 H. Sawada, N. Nishimura, E. Suzuki, J. Zhuang, K. Hasegawa, H. Takamatsu, K. Honda and K. Hasumi, *J. Cereb. Blood Flow Metab.*, 2014, **34**, 235–241.